HHS Public Access

Author manuscript

J Immunol. Author manuscript; available in PMC 2022 June 15.

Published in final edited form as:

J Immunol. 2021 June 15; 206(12): 2966–2979. doi:10.4049/jimmunol.2001468.

Knockout of *MAPK phosphatase-1* Exaggerates Type I Interferon Response during Systemic *Escherichia coli* Infection

Sean G. Kirk[*], **Parker R. Murphy**[*], **Xiantao Wang**[†], **Charles J. Cash**[*], **Timothy J. Barley**[*], **Bridget A. Bowman**[*], **Abel J. Batty**[*], **William E. Ackerman IV**[‡], **Jian Zhang**[¶], **Leif D. Nelin**[*,§], **Markus Hafner**[†], **Yusen Liu**[*,§,2]

[*]Center for Perinatal Research, The Research Institute at Nationwide Children's Hospital, Columbus, OH 43215, USA

[†]Laboratory of Muscle Stem Cells and Gene Regulation, National Institute of Arthritis and Musculoskeletal and Skin Disease, National Institutes of Health, Bethesda, MD 20892, USA

[‡]Department of Obstetrics & Gynecology, University of Illinois at Chicago College of Medicine, Chicago, IL 60612, USA

[§]Department of Pediatrics, The Ohio State University College of Medicine, Columbus, OH 43205, USA

[¶]Department of Pathology, University of Iowa Carver College of Medicine, Iowa City, IA 52242, USA

Abstract

We have previously shown that *Mkp-1*-deficient mice produce elevated TNF-α, IL-6, and IL-10 following systemic *E. coli* infection, and exhibited increased mortality, elevated bacterial burden, and profound metabolic alterations. To understand the function of Mkp-1 during bacterial infection, we performed RNA-seq analysis to compare the global gene expression between *E. coli*-infected wildtype and *Mkp-1*$^{-/-}$ mice. A large number of interferon-stimulated genes were more robustly expressed in *E. coli*-infected *Mkp-1*$^{-/-}$ mice than in wildtype mice. Multiplex analysis of the serum cytokine levels revealed profound increases in IFN-β, IFN-γ, TNF-α, IL-1α and β, IL-6, IL-10, IL-17A, IL-27, and GMSF levels in *E. coli*-infected *Mkp-1*$^{-/-}$ mice relative to wildtype mice. Administration of a neutralizing antibody against the receptor for type I IFN to *Mkp-1*$^{-/-}$ mice prior to *E. coli* infection augmented mortality and disease severity. *Mkp-1*$^{-/-}$ bone marrow-derived macrophages (BMDM)[3] produced higher levels of IFN-β mRNA and protein, than did wildtype BMDM upon treatment with LPS, *E. coli*, poly(I:C), and herring sperm DNA. Augmented IFN-β induction in *Mkp-1*$^{-/-}$ BMDM was blocked by a p38 inhibitor, but not by an JNK inhibitor. Enhanced Mkp-1 expression abolished IFN-β induction by both LPS and *E. coli* but had little effect on the *IFN-β* promoter activity in LPS-stimulated RAW264.7 cells. *Mkp-1* deficiency did not have an overt effect on IRF3/7 phosphorylation or IKK activation but modestly enhanced IFN-β mRNA stability in LPS-stimulated BMDM. Our results suggest that Mkp-1

[2]Address correspondence and reprint requests to Professor Yusen Liu, Center for Perinatal Research, The Abigail Wexner Research Institute at Nationwide Children's Hospital, 575 Children's Cross Road, Columbus, OH 43215. yusen.liu@nationwidechildrens.org.

regulates IFN-β production primarily through a p38-mediated mechanism and that IFN-β plays a beneficial role in *E. coli*-induced sepsis.

Introduction

The innate immune system acts as the first line of defense against invading bacterial pathogens (1). Mammals rely on germ line encoded pattern recognition receptors to detect bacterial components (2, 3). Recognition of the bacterial components activates a cascade of signaling events leading to activation of MAPK pathways and key transcription factors such as NF-κB (4–8). These transcription factors cooperate to initiate a transcriptional program by enhancing the expression of a variety of immune-related proteins including pro-inflammatory cytokines, chemokines, and anti-inflammatory cytokines (7, 9). Some of the cytokines promote leukocyte recruitment and enhance cellular and humoral bactericidal activities (10–14), while others restrain inflammation and limit the collateral damage to the host (15).

MAPK phosphatase (Mkp)-1, also referred to as DUSP1 (16), CL100 (17), 3CH134 (18), and Erp (19), is a dual specificity protein phosphatase that preferentially acts on p38 and JNK MAPK subfamilies (20, 21). In innate immune cells Mkp-1 is robustly induced in response to bacterial infection, and serves as a negative regulator of the innate immune response (22, 23). We and others have shown that *Mkp-1*-deficient macrophages produce considerably greater amounts of cytokines including TNF-α, IL-6, and IL-10 than do wildtype macrophages in vitro (24–29). Manetsch et al. found that knockdown of MKP-1 in TNF-α-stimulated human airway muscle cells enhanced both p38 and JNK activity and augmented IL-8 production (30), illustrating the importance of MKP-1 in the control of secondary inflammatory responses in stromal/parenchymal cells. In an *E. coli*-induced sepsis model, *Mkp-1*$^{-/-}$ mice also produced markedly greater levels of cytokines such as TNF-α, IL-6, and IL-10, and exhibited increased mortality (31). Increased bacterial burden, more severe organ damage, and metabolic abnormalities were also observed in *Mkp-1*$^{-/-}$ mice relative to wildtype mice after *E. coli* infection (31, 32). To understand the pathophysiology that *Mkp-1*$^{-/-}$ mice exhibit after systemic *E. coli* infection, we performed multiplex analysis of the serum cytokines in *E. coli*-infected wildtype and *Mkp-1*$^{-/-}$ mice. We observed enhanced cytokine production in *Mkp-1*$^{-/-}$ mice for 10 of the 13 cytokines tested. Among the cytokines enhanced by Mkp-1 deficiency in *E. coli*-infected mice is interferon (IFN)-β, a type I IFN critical for host defense against viral infections (33–35). While regulation of IFN-β induction by TANK-binding kinase 1 (TBK1) mediated interferon regulatory factors (IRFs) and NF-κB during viral infections has been well studied (36–40), the regulation of IFN-β by Mkp-1 has not been fully understood, particularly in the context of bacterial infection. Type I interferon has been shown to play both beneficial and detrimental roles during bacterial infections, depending on the pathogens and mode of infections (41–43). We found that concurrent with a greater increase in IFN-β levels in the blood, many interferon-inducible genes were more robustly induced in *Mkp-1*$^{-/-}$ mice than in *Mkp-1*$^{+/+}$ mice following *E. coli* infection. To address the role of Mkp-1 in the regulation of type I interferon, we studied the mechanism underlying Mkp-1-mediated regulation in macrophages using *Mkp-1* knockout and over-expressing cells as well as pharmacological

inhibitors. We also studied the physiological role of IFN-β during *E. coli* infection in *Mkp-1*$^{-/-}$ mice by using an IFN-α/β receptor 1 (IFNAR1) neutralizing antibody. Our studies indicate that Mkp-1 regulates IFN-β expression through controlling p38 but not JNK and IFN-β induction is beneficial for the host during *E. coli* infection.

Materials and Methods

Experimental animals

Mkp-1$^{-/-}$ mice have been described previously (25, 44) and have no obvious phenotype prior to experimental use. *Mkp-1*$^{+/-}$ mice on a C57/129 mixed background were generously provided by Bristol-Myers Squibb Pharmaceutical Research Institute (Princeton, NJ). *Mkp-1*$^{+/-}$ mice were intercrossed to generate *Mkp-1*$^{-/-}$ and *Mkp-1*$^{+/+}$ mice for *E. coli* infection experiments. Additionally, the *Mkp-1*$^{+/-}$ mice were backcrossed to C57BL/6J mice for 8 generations to create *Mkp-1*$^{-/-}$ mice on a C57BL/6J background. While *Mkp-1*$^{-/-}$ and *Mkp-1*$^{+/+}$ mice on C57/129 background were used for all infection experiments, all macrophage studies in vitro were carried out using bone marrow isolated from the mice on C57BL/6J background. All mice were housed with a 12 h alternating light-dark cycle at 25°C, with humidity between 30% and 70%, and have access to food and water ad libitum. All experiments were performed according to National Institutes of Health guidelines and were approved by the Institutional Animal Care and Use Committee at the Research Institute at Nationwide Children's Hospital.

E. coli infection

A wild-type (smooth) strain of *E. coli* (O55:B5, ATCC 12014) was purchased from American Tissue Culture Collection (Manassas, VA). Bacteria were grown in nutrient broth for 18 h at 37°C and refreshed by culturing in new medium for 2 h after a 1:5 dilution. Bacteria were washed three times with sterile PBS and adjusted to the appropriate final concentration. The bacterial suspension was injected into the tail vein of the mice at the volume of ~250 μl per mouse, as previously described (31, 32). Mouse survival was monitored for 7 days. In the antibody neutralization experiments, mice were first given i.p. 100 μg of In Vivo Plus murine monoclonal anti-mouse IFNAR1 antibody (Catalog#: BP0241) or In Vivo Plus mouse IgG1 isotype control antibody (Catalog#: BP0083) purchased from BioXCell (Lebanon, NH). The mice were then infected with *E. coli* i.v. 1 h later. Mortality was monitored over seven days. Disease severity was assessed using a sepsis morbidity scoring system (Table I), which was adopted and refined from the murine sepsis score system developed by Shrum et al (45). This score system evaluates morbidity in seven categories: appearance, level of consciousness, activity, response to stimuli, eye state, respiration rate and quality. Each of these categories was given a score between 0 and 4. The individual scores in all categories were added together to yield the total score for a specific animal at the time of examination. Mice that died or were in moribundity (euthanized) at the time of evaluation were given a maximal score of 28.

Bacterial load determination

Bacterial burden was determined 24 h after infection as previously described (31). Bacterial colonies were counted separately for each sample. Spleen samples were normalized to organ weight and blood samples were normalized to blood volume.

Generation of expression heat map of interferon-stimulated genes

Mkp-1$^{+/+}$ and *Mkp-1*$^{-/-}$ mice were infected i.v. with *E. coli* at the dose of 2.5×10^7 CFU/g body weight (b.w.). Livers were isolated 24 h post infection, and total RNA was isolated from 4 animals in each treatment group for RNA-seq analysis (32). The RNA-seq data have been deposited in Gene Expression Omnibus (GSE122741). A comprehensive list of 71 known interferon-stimulated genes was compiled, and the transcript copy numbers were used to calculate the fold of changes and p values using a t-test. The fold change of transcripts for each gene was calculated relative to the average expression in control *Mkp-1*$^{+/+}$ mice (injected with PBS, i.v.). The data set was then sorted from the highest level to the lowest level. Values were $\log_2$-transformed to generate a heat-map where red indicates up-regulation, white indicates no change, and blue indicates down-regulation of gene expression.

ELISA and multiplex assessment for cytokines

Interferon concentrations in blood and cell culture medium were measured by ELISA following a standard protocol (46) with minor modifications. Briefly, wells on 96-well plates were coated with an IFN-β-capture antibody (Catalog number 519202, BioLegend, San Diego, CA) diluted in phosphate-buffered saline overnight at 4°C. The wells were washed 3 times with PBS, and then blocked with ELISA diluent (PBS containing 10% FBS) for 1 h at room temperature. Subsequently, the wells were washed 3 times with PBS, and the adequately diluted samples (serum or cell culture media) and mouse IFN-β standard (BioLegend) were added into the wells to allow incubation at room temperature for 2 h. The samples were aspirated, and the wells were washed 5 times with PBS. The detection antibody (Catalog #: 32400–1, PBL Assay Science, Piscataway, NJ) diluted to a concentration of 50 neutralization units per ml was added to the wells and allowed to incubate at room temperature for 1 h. After 5 washes with PBS, HRP-conjugated goat anti-rabbit IgG (Catalog number: 111-035-144, Jackson ImmunoReasearch, West Grove, PA) diluted by 5,000-fold in PBS containing 10% FBS was added to the wells and allowed to incubate for 30 min at room temperature. After 7 washes with PBS, color was developed using 1× 3,3’,5,5’-tetramethylbenzidine solution (Pierce, Rockford, IL) and the absorbance was measured at 450 nm, using the SpectraMax M2 microplate reader (Molecular Devices, Sunnyvale, CA). The IFN-β concentration was calculated based on the standard curve using the SoftMax pro program (Molecular Devices).

Multiplex cytokine assessment for mouse sera was carried out using a LEGENDplex multiplex kit (BioLegend) according to the manufacturer’s recommendations. We used a pre-defined mouse inflammation panel to quantify 13 mouse cytokines (GM-CSF, IFN-β, IFN-γ, IL-1α, IL-1β, IL-6, IL-10, IL-12 p70, IL-17A, IL-23, IL-27, MCP-1, and TNF-α).

Macrophage derivation, culture, and stimulation

Bone marrow was isolated from *Mkp-1*$^{+/+}$ and *Mkp-1*$^{-/-}$ mice on the C57BL/6J background, and the red blood cells were lysed by incubating in ACK lysing buffer (Invitrogen, Carlsbad, CA) for 2–3 min. The remaining bone marrow cells were cultured on petri dishes in DMEM supplemented with 10% FBS (Atlantic Biologicals, Flowery Branch, GA), 25% L929-conditioned medium, 10 mM HEPES Buffer, 100 units/ml penicillin, 100 μg/ml streptomycin, and 10 μg/ml gentamicin (Invitrogen). The cells were re-fed once with fresh medium after 4 days and cultured for 3 additional days to generate bone marrow-derived macrophages (BMDM).

BMDM were stimulated with LPS (O55:B5) (Calbiochem, San Diego, CA) or heat-killed *E. coli* for different times. Stimulation of BMDM with synthetic dsRNA polyinosinic:polycytidylic acid (poly (I:C)) (Invivogen, San Diego, CA) and sonicated herring sperm DNA (Sigma-Aldrich, St. Louis, MO, USA) was carried out by transfection with polyethylenimine (Polysciences, Warrington, PA), as previously described (47). In some experiments, BMDM were pre-treated with either vehicle (DMSO) or a pharmacological inhibitor of p38 (SB203580 (48), Calbiochem) or JNK (JNK-IN-8 (49), Selleck Chemicals, Houston, TX) for 15 min prior to TLR ligand or *E. coli* stimulation. Medium was harvested for ELISA and cells were lysed to harvest proteins for Western blot analysis, or to harvest total RNA for quantitative RT-PCR (qRT-PCR) as previously described (50).

RAW264.7 cells culture, transfection, and luciferase assays

RAW264.7 cells were modified using the PiggyBac expression system (51) (SBI System Biosciences, La Jolla, CA) to express rat Mkp-1 protein under a tetracycline-inducible (Tet-ON) promoter (52). We incorporated the one-vector tetracycline-inducible expression feature of the plasmid pCW57.1 MCS1-P2A-MCS2 (neo) (53) into the PiggyBac vector to create a new vector PB-SK2. The PB-SK2 vector carries two tandem expression cassettes sandwiched by two specific inverted terminal repeats (ITRs). The first cassette expresses reverse tetracycline-controlled transactivator (rtTA) and the neomycin phosphotransferase separated by a Thosea asigna virus 2A peptide bond skipping sequence. The second expression cassette harbors a transgene under a promoter containing 5 tetracycline response elements. In the presence of doxycycline, the rtTA transcription factor generated by the first expression cassette will turn on the expression of the transgene in the second expression cassette. The neomycin phosphotransferase confers G418 resistance to the cells. When co-transfected with a hyperactive PiggyBac transposase vector, the transposase can bind to the specific ITRs of the Piggybac vector and excise the ITR-flanked expression cassettes, and insert into the genome at TTAA sites (51). We cloned the rat Mkp-1 cDNA into the EcoRI site downstream of the TRE promoter. The authenticity of the constructs was confirmed by DNA sequencing. The empty Piggybac vector PB-SK2 or PB-SK2 containing the rat Mkp-1 cDNA was co-transfected with a hyperactive PiggyBac transposase vector (51) into RAW264.7 cells, using lipofectamine 3000 (Invitrogen). After transfection, the cells were selected for 2 weeks in medium containing 500 μg/ml G418. Individual clones were isolated to test for the expression of Mkp-1 in the absence and presence of doxycycline. The leftover clones were pooled. Adequate RAW264.7 derivative clones and the pools were maintained

in DMEM supplemented with 10% FBS, 100 units/ml penicillin, 100 μg/ml streptomycin, and 150 μg/ml G418 (Invitrogen). These cells were cultured in medium with or without doxycycline overnight, and then stimulated with heat-killed *E. coli* or LPS to harvest cell lysates for Western blot analysis or collect culture medium for ELISA.

In the luciferase assay experiment, we transfected RAW264.7 cell clone (clone 22), which was stably integrated with a Tet-ON Mkp-1 expression cassette, with a hyperactive PiggyBac transposase vector and a PiggyBac vector carrying a luciferase reporter linked to the proximal mouse *IFN-β* promoter (nucleotides −53 to −195) (54). The cells were then selected with puromycin for 2 weeks. The cell pool was then treated with doxycycline (100 ng/ml) overnight or left untreated. These cells were then stimulated with LPS or heat-killed *E. coli* for 6 h or left unstimulated. Cells were then washed with PBS and lysed to measure luciferase activity in the cell lysates, using a Renilla luciferase assay system (Promega, Madison, WI), according to the manufacturer's recommendations.

Western blot analysis

Western blot analysis was carried out as previously described (24, 55). The rabbit monoclonal antibodies against phosphor-IRF3 (Ser396), total IRF3, phosphor-IRF7 (Ser437/538), phosphor-TBK1 (Ser172), total TBK1, phosphor-IκB kinase (IKK) α/β (Ser176/180), and Mkp-1 were purchased from Cell Signaling (Danvers, MA, USA). The mouse monoclonal antibodies against radical S-adenosyl methionine domain containing 2 (Rsad2), interferon-stimulated gene (Isg) 15, IκBα, and fatty acid synthase (Fasn) as well as the polyclonal antibody against IKKα/β were purchased from Santa Cruz Biotechnology (Dallas, Texas, USA). The mouse monoclonal antibody against β-actin was purchased from Sigma-Aldrich. The immunoblots were stripped and re-probed with an antibody against a house-keeping protein to control for loading. Western blots were developed using chemiluminescent reagent ECL Immobilon (Millipore Corporation, Billerica, MA). Western blot images were acquired using Epson Perfection 4990 PHOTO scanner (Epson, Long Beach, CA, USA).

Assessment of IFN-β mRNA expression and stability

BMDM were stimulated with heat-killed *E. coli* (O55:B5, ATCC 12014) or various TLR ligands for different amounts of time. For *E. coli* stimulation, heat-killed *E. coli* were added to cell culture plates at a ratio of 10 bacteria per macrophage, and then the plates were centrifuged in swinging buckets for 2 min at 2,000 rpm at 37°C. Total RNA samples were harvested from the cells using Trizol. Genomic DNA was removed by digesting the total RNA with RQ1 RNase-Free DNase (Promega, Madison, WI). Liver RNA was then reverse transcribed on a PTC-200 DNA Engine Cycler (Bio-Rad, Hercule, CA) with High-Capacity cDNA Reverse Transcription Kit (Applied Biosystems, Foster City, CA). qRT-PCR was performed using PowerUp SYBR Green PCR Master Mix (Applied Biosystems) on a Realplex^2 Mastercycler (Eppendorf, Hauppauge, NY).

For measuring IFN-β mRNA decay, BMDM were stimulated with heat-killed *E. coli* for 2 h. Actinomycin D was added into the culture medium at a concentration of 5 μg/ml. Total RNA was harvested from the cells using Trizol (Invitrogen)

after 0, 2, 4, and 8 h. IFN-β mRNA levels were quantified by qRT-PCR to assess IFN-β mRNA decay using primers 5'-GCCAGGAGCTTGAATAAAATG-3' and 5'-GATGGTCCTTTCTGCCTCAG-3', as previously described (46, 47). 18S ribosomal RNA was detected using 5'-GTAACCCGTTGAACCCCATT-3' and 5'-CCATCCAATCGGTAGTAGCG-3' and used as an internal control for normalization. The levels of IFN-β mRNA expression was calculated relative to 18S using the $2^{-\Delta\Delta CT}$ method (36).

Statistical analyses

Survival differences between groups were analyzed by Kaplan-Meier analysis with log-rank test using the on-line statistics program (http://www.obg.cuhk.edu.hk/ResearchSupport/StatTools/Survival_Pgm.php) developed by Dr. Allan Chang, Department of Obstetrics and Gynaecology, Chinese University of Hong Kong. Differences in cytokine production or gene expression between groups were compared using t-test or two-way ANOVA with GraphPad Prism 8.2.0 program (GraphPad Software, San Diego, CA). A value of $p<0.05$ was considered statistically significant for all analyses.

Results

Mkp-1$^{-/-}$ mice produce significantly greater IFN-β and have a substantially enhanced interferon signature in global gene expression in the liver

Previously, we have found that *Mkp-1*$^{-/-}$ mice exhibited a profound defect in host defense against *E. coli* infection, indicated by substantial increases in mortality, bacterial burden, and organ damage associated with increased production of TNF-α, IL-6, and IL-10 compared to wildtype mice. To gain insight into the physiological function of *Mkp-1* in sepsis after systemic *E. coli* infection, we analyzed the RNA-seq datasets (GSE122741) generated using livers of control and *E. coli*-infected *Mkp-1*$^{+/+}$ and *Mkp-1*$^{-/-}$ mice (32). We noticed a profound enhancement of an IFN genetic response signature, although neither type I IFN nor type II IFN mRNA(s) were expressed in the livers of these mice. Interferons evoke a unique genetic program via inducing the expression of many interferon-stimulated genes (Isgs). We compiled the mRNA transcript levels of all known interferon-stimulated genes that were expressed in the livers (Table S1), log-transformed the values, and generated a heatmap (Figure 1). Nearly 60 of the 71 interferon-stimulated genes were up-regulated in *Mkp-1*$^{+/+}$ mice upon *E. coli* infection. Forty of the 71 interferon-stimulated genes, including myxovirus resistance (Mx) 1, Mx2, 2'−5'-oligoadenylate synthase-like protein 1 (Oasl1), Rsad2, nicotinamide phosphoribosyltransferase (Nampt), interferon-stimulated gene (Isg) 15, Isg20, and ubiquitin specific peptidase 18 (Usp18), were expressed at higher levels in *Mkp-1*$^{-/-}$ mice than in *Mkp-1*$^{+/+}$ mice following *E. coli* infection. Western blot analysis confirmed the enhanced protein expression for Rsad2 (Figs. 2A, 2B) but not Isg15 (Fig. 2C), suggesting that the transcription of these interferon-regulated genes is not the only mechanism controlling their protein levels.

Mkp-1 deficiency enhances the production of a large number of cytokines, including both IFN-β and IFN-γ

To understand the molecular basis for the enhanced IFN signature in *E. coli*-infected *Mkp-1*$^{-/-}$ mice, we measured the levels of 13 cytokines, including IFN-β, IFN-γ, TNF-α, IL-1α, IL-1β, IL-6, IL-10, IL-12p70, IL-17A, IL-23, IL-27, MCP-1, and GM-CSF, in the sera of *Mkp-1*$^{+/+}$ and *Mkp-1*$^{-/-}$ mice prior and following *E. coli* infection. We infected *Mkp-1*$^{+/+}$ and *Mkp-1*$^{-/-}$ mice i.v. with *E. coli* (2.5×10^7 CFU/g b.w.) and analyzed the cytokine levels after 3, 6, or 24 h using a multiplex cytokine assay kit. As previously described (31), *Mkp-1*$^{-/-}$ mice produced substantially more TNF-α, IL-6, and IL-10 than did *Mkp-1*$^{+/+}$ mice following *E. coli* infection at all three time points (Figs. 3A–C). The differences in IL-6 and IL-10 at 24 h were particularly striking. While IL-6 and IL-10 returned to close to basal levels in *Mkp-1*$^{+/+}$ mice at 24 h, IL-6 and particularly IL-10 levels remained at very high levels in *Mkp-1*$^{-/-}$ mice at 24 h. At this point, the IL-6 and IL-10 levels in *Mkp-1*$^{-/-}$ mice were 3- and 31-fold higher than in *Mkp-1*$^{+/+}$ mice, respectively. In addition, IL-17A and IL-27 production in *Mkp-1*$^{-/-}$ mice were also dramatically increased relatively to *Mkp-1*$^{+/+}$ mice following *E. coli* infection at both early and late time points (Figs. 3D, 3E). Interestingly, three cytokines, IL-1α, IL-1β, and GM-CSF, were similar in the two groups of mice at early time points (3 and 6 h) post-infection but diverged in different directions by 24 h (Figs. 3F–H). At that point, the levels of these cytokines were substantially decreased in *Mkp-1*$^{+/+}$ mice, but further increased (such as IL-1α) or persisted at the peak levels (GM-CSF and IL-1β) in *Mkp-1*$^{-/-}$ mice. Although serum MCP-1 levels were dramatically increased in both *Mkp-1*$^{+/+}$ and *Mkp-1*$^{-/-}$ mice following *E. coli* infection, there was no significant difference between the two groups of *E. coli*-infected mice (data not shown). IL-23 levels did not change in either *Mkp-1*$^{+/+}$ or *Mkp-1*$^{-/-}$ mice after *E. coli* infection (data not shown). IL-12p70 levels were only slightly increased in *Mkp-1*$^{-/-}$ mice after *E. coli* infection, and there were no differences between the two groups of *E. coli*-infected mice (data not shown). Interestingly, the levels of IFN-γ were very low in uninfected mice, but dramatically increased 6 h after *E. coli* infection in both *Mkp-1*$^{+/+}$ and *Mkp-1*$^{-/-}$ mice (Fig. 3I). Although IFN-γ levels in *Mkp-1*$^{-/-}$ mice were significantly higher than in *Mkp-1*$^{+/+}$ mice 6 h after *E. coli* infection, IFN-γ levels in the *Mkp-1*$^{+/+}$ mice plummeted to nearly basal levels by 24 h. In contrast, elevated levels of IFN-γ in *E. coli*-infected *Mkp-1*$^{-/-}$ mice persisted at 24 h post infection. Although IFN-β levels in *Mkp-1*$^{+/+}$ mice did not significantly change, IFN-β levels at both 3 h and 24 h post *E. coli* infection in *Mkp-1*$^{-/-}$ mice were significantly higher than in infected *Mkp-1*$^{+/+}$ mice (Fig. 3J). We also developed a sandwich ELISA assay in house to verify the observed differences in serum IFN-β levels between *E. coli*-infected *Mkp-1*$^{+/+}$ and *Mkp-1*$^{-/-}$ mice (Fig. 3K). The ELISA assays showed that IFN-β production was induced by *E. coli* infection in both *Mkp-1*$^{+/+}$ and *Mkp-1*$^{-/-}$ mice. Although blood IFN-β levels in uninfected *Mkp-1*$^{+/+}$ and *Mkp-1*$^{-/-}$ mice were comparable, serum IFN-β levels 24 h after *E. coli* infection were over 3-fold higher in *Mkp-1*$^{-/-}$ mice than in *Mkp-1*$^{+/+}$ mice (Fig. 3K).

Neutralizing IFN-β in Mkp-1$^{-/-}$ mice exacerbates the severity of disease following E. coli infection

To address the significance of elevated type I IFN, IFN-β, in the phenotype of *Mkp-1*$^{-/-}$ mice during *E. coli* infection, we blocked IFNAR1 with a neutralizing antibody, and

documented survival (Fig. 4). While prophylactic neutralizing IFNAR1 with a monoclonal antibody appeared to increase mortality, the difference compared to the mortality after treatment with an isotype control antibody did not reach statistical significance. We then assessed the effect of IFNAR1 blockade on disease severity using a comprehensive murine sepsis scoring system (Table I) that evaluates appearance, consciousness, activity, response to stimuli, eyes, respiratory rate and quality. We found that the IFNAR1 neutralizing antibody augmented disease severity in *Mkp-1*$^{-/-}$ mice following *E. coli* infection (Fig. 4B). Neutralization of IFNAR1 by the antibody almost completely abolished the increase in liver Rsad2 protein level in *Mkp-1*$^{-/-}$ mice triggered by *E. coli* infection (Fig. 4C), confirming the blockade of type I IFN signaling in mice received the IFNAR1-neutralizing antibody. To our surprise, IFNAR1 neutralization had neither a significant effect on serum TNF-α or IL-6 levels (Fig. 4D), nor affected bacterial burdens in the blood or spleens (Fig. 4E). These results demonstrate that increased IFN-β is actually beneficial to the mice, suggesting that exacerbating IFN-β production is not responsible for the enhanced mortality and bacterial burden of *Mkp-1*$^{-/-}$ mice after *E. coli* infection.

Mkp-1 negatively regulates IFN-β production

To delineate the molecular mechanism by which Mkp-1 regulates IFN-expression, we analyzed the effects of Mkp-1 on IFN-β production in macrophages. First, we compared IFN-β production in *Mkp-1*$^{+/+}$ and *Mkp-1*$^{-/-}$ BMDM following stimulation with heat-killed *E. coli* (Fig. 5A). While *E. coli* stimulation resulted in IFN-β production in *Mkp-1*$^{+/+}$ BMDM, substantially more IFN-β (>5-fold) was produced by *Mkp-1*$^{-/-}$ BMDM following *E. coli* stimulation than by *Mkp-1*$^{+/+}$ BMDM. As LPS is an important pathogenic factor in Gram-negative bacteria and a potent stimulant for IFN-β production (56), we assessed the effect of Mkp-1 deficiency on LPS-stimulated IFN-β production (Fig. 5B). Similar to what was observed in *E. coli*-stimulated BMDM, Mkp-1 deficiency substantially enhanced IFN-β production in LPS-stimulated BMDM.

We then assess the effect on Mkp-1 deficiency on IFN-β mRNA levels in *E. coli*-stimulated BMDM by qRT-PCR (Fig. 5C). *E. coli* stimulation resulted in an ~400-fold increase in IFN-β mRNA levels at 1 h in *Mkp-1*$^{+/+}$ BMDM, followed by a gradual decrease such that by 6 h post stimulation, IFN-β levels were ~40-fold above basal levels. The increase in IFN-β mRNA levels was dramatically enhanced in *Mkp-1*$^{-/-}$ BMDM. Following *E. coli* stimulation, IFN-β mRNA levels increased to >2,000-fold over the basal level in *Mkp-1*$^{+/+}$ macrophages within 1 h. IFN-β mRNA levels maintained and slightly increased at 2 h, and then rapidly declined.

We also assessed whether over-expression of Mkp-1 inhibits IFN-β production. We established stable RAW264.7 clones (clones 15, 13, 21, 22) that express the rat Mkp-1 protein in a doxycycline-inducible manner. RAW264.7 is a macrophage-like mouse cell line that can produce a variety of cytokines in response to pathogenic stimulation (57). Doxycycline treatment dramatically increased Mkp-1 expression in these cells (Fig. 6A, Upper panel). It is worth noting that in the absence of doxycycline these Mkp-1-inducible RAW264.7 clones exhibited an elevated basal Mkp-1 level that was comparable to the endogenous Mkp-1 level 1 h after LPS stimulation in the parental RAW264.7 cells (Fig.

6A, Middle panel). Interestingly, LPS stimulation further increased the levels of Mkp-1 expression in these clones. Importantly, doxycycline treatment substantially inhibited IFN-β production in two of the tested Mkp-1-expressing clones (clones 15 and 22) following both LPS and *E. coli* stimulation (Fig. 6B). As there were substantial variability between the individual cell clones (Fig. 6B, note the differences in scales of the y-axis between clone 15 and clone 22), we assessed IFN-β production using pools of the stable doxycycline-inducible clones. In the stable RAW264.7 pool transfected with an empty vector, both *E. coli* and LPS triggered a substantial increase in IFN-β production, and doxycycline pre-treatment has no effect on IFN-β production (Fig. 6C, Left graph). In contrast, in the pool stably transfected with the Tet-ON Mkp-1 plasmid, doxycycline-induced Mkp-1 expression dramatically inhibited IFN-β production, although IFN-β production was potently stimulated by either *E. coli* or LPS in the absence of doxycycline (Fig. 6C, Right graph).

The pharmacological inhibitor of p38, but not JNK, blocks IFN-β expression

Mkp-1 prefers p38 and JNK as substrates (21), and Mkp-1 deficiency resulted in a considerable prolongation of p38 and JNK activity in BMDM following LPS stimulation (26–29). We assessed whether p38 and JNK are involved in the production of IFN-β in BMDM stimulated with *E. coli* and other TLR ligands. First, we assessed the effects of p38 and JNK inhibition on the production of IFN-β in BMDM stimulated with *E. coli* and LPS. Pre-treatment of BMDM with a pharmacological inhibitor of p38, SB203580, substantially attenuated IFN-β production in both *Mkp-1*$^{+/+}$ and *Mkp-1*$^{-/-}$ BMDM stimulated with *E. coli* (Fig. 7A). Although the JNK inhibitor, JNK-IN-8, alone had little effect, combination of both SB203580 and JNK-IN-8 had a greater inhibitory effect on *E. coli*-induced IFN-β production than did SB203580 alone in *Mkp-1*$^{-/-}$ BMDM but not in *Mkp-1*$^{+/+}$ BMDM (Fig. 7A). While SB203580 substantially inhibited LPS-stimulated IFN-β production in both *Mkp-1*$^{+/+}$ and *Mkp-1*$^{-/-}$ BMDM, JNK-IN-8 had little effect (Fig. 7B). The addition of both JNK-IN-8 and SB203580 did not significantly enhance the inhibition of SB203580 alone on LPS-induced IFN-β production in either *Mkp-1*$^{-/-}$ or *Mkp-1*$^{+/+}$ BMDM. These results clearly demonstrate that p38 is primarily responsible for the dramatic increase in IFN-β in stimulated *Mkp-1*$^{-/-}$ BMDM.

We then assessed the effect of p38 inhibition on kinetics of IFN-β production and IFN-β mRNA induction following *E. coli* stimulation. *E. coli*-induced IFN-β levels in the medium increased gradually over a 6-h period for both *Mkp-1*$^{+/+}$ and *Mkp-1*$^{-/-}$ BMDM, although the increase was substantially greater for *Mkp-1*$^{-/-}$ BMDM (Fig. 7C). The increase in *E. coli*-induced IFN-β levels were detected within 2 h. IFN-β reached a peak level at ~4 h in *Mkp-1*$^{+/+}$ BMDM, while IFN-β levels continued to increase for 6 h in *Mkp-1*$^{-/-}$ BMDM. Pre-treatment of both *Mkp-1*$^{+/+}$ and *Mkp-1*$^{-/-}$ BMDM with SB203580 almost completely abolished *E. coli*-induced IFN-β production in both groups. IFN-β mRNA reached peak levels at 1–2 h in both *Mkp-1*$^{+/+}$ and *Mkp-1*$^{-/-}$ BMDM following *E. coli* stimulation, then declined, although IFN-β mRNA reached substantially greater levels in *Mkp-1*$^{-/-}$ BMDM (Fig. 7D). SB203580 pre-treatment decreased IFN-β mRNA levels substantially in both *Mkp-1*$^{+/+}$ and *Mkp-1*$^{-/-}$ BMDM. We also assessed the effect of SB203580 on IFN-β mRNA induction in *Mkp-1*$^{+/+}$ and *Mkp-1*$^{-/-}$ BMDM treated with LPS, poly (I:C), or herring sperm

DNA. LPS and poly (I:C) activate TLR4 (58) and TLR3 (59), respectively. Poly (I:C) is also recognized by cytosolic pathogen sensor RIG-I (60). Herring sperm double-stranded DNA has been shown to activate the cyclic GMP-AMP synthase (cGAS)-Stimulator of interferon genes (STING) pathway to stimulate IFN-β expression (61). Similar to what was seen in cells stimulated with *E. coli*, LPS-stimulated IFN-β mRNA expression in *Mkp-1*$^{+/+}$ and *Mkp-1*$^{-/-}$ BMDM was abolished by SB203580 (Fig. 7E). SB203580 also abolished IFN-β mRNA induction by transfection of either poly (I:C) or herring sperm DNA in both *Mkp-1*$^{+/+}$ and *Mkp-1*$^{-/-}$ BMDM (Fig. 7F). These results further highlight the critical role of p38 in the regulation of IFN-β induction during pathogenic infections.

Since p38 controls the production of many cytokines via regulating the stability of cytokine mRNAs, we assessed whether IFN-β mRNA stability is affected by Mkp-1 deficiency. BMDM were stimulated with heat-killed *E. coli* for 2 h, and then treated with actinomycin D to stop gene transcription. Cells were harvested at different times, and IFN-β mRNA levels in these samples were assessed by qRT-PCR (Fig. 8A). Half-life of IFN-β mRNA was calculated based on the rate of mRNA decay. The half-life of IFN-β mRNA in *Mkp-1*$^{+/+}$ macrophages was ~4.1 h, while the half-life in *Mkp-1*$^{-/-}$ macrophages was moderately longer, ~5.9 h, suggesting that enhanced IFN-β mRNA stability contributes to the elevated IFN-β expression in *Mkp-1*$^{-/-}$ macrophages.

To address whether Mkp-1 affects IFN-β gene transcription, we stably integrated an *IFN-β*-luciferase reporter into an RAW264.7 cell line harboring a Tet-ON Mkp-1 expression cassette. Cells were treated with doxycycline overnight or left untreated, and then stimulated with LPS or heat-killed *E. coli* for 6 h prior to harvesting for luciferase activity assays (Fig. 8B). Doxycycline treatment had no effect on the *IFN-β*-luciferase reporter in both unstimulated and LPS-stimulated cells, indicating that elevated Mkp-1 expression did not affect LPS-stimulated *IFN-β* promoter activity. However, doxycycline treatment slightly decreased *IFN-β*-luciferase reporter activity in *E. coli*-induced cells by approximately 20%, indicating a slight inhibition on *IFN-β* promoter activity.

IFN-β transcription is regulated by multiple transcription factors, including IRF3, IRF7, and NF-κB, through phosphorylation mediated by protein kinases (62, 63). We compared IRF3 and IRF7 phosphorylation in *Mkp-1*$^{+/+}$ and *Mkp-1*$^{-/-}$ BMDM after LPS stimulation by Western blotting using phosphor-specific antibodies (Fig. 8C). IRF3 was rapidly phosphorylated in both *Mkp-1*$^{+/+}$ and *Mkp-1*$^{-/-}$ BMDM following LPS stimulation, and there was no overt difference in the kinetics or magnitude of IRF3 phosphorylation between these cells. Phosphorylation of IRF7 was similar. We then assessed the activities of upstream kinases using phosphor-specific antibodies (Fig. 8D). LPS stimulation led to a transient TBK1 phosphorylation/activation in both *Mkp-1*$^{+/+}$ and *Mkp-1*$^{-/-}$ BMDM. TBK1 phosphorylation reached peak level at 30–90 min, and substantially declined by 3 h post LPS stimulation. There was no overt difference in TBK1 phosphorylation between the two groups. Activation of IKKα/β occurred within 15 min after LPS stimulation, and then IKKα/β phosphorylation rapidly declined. No obvious difference in IKKα/β activity was observed between *Mkp-1*$^{+/+}$ and *Mkp-1*$^{-/-}$ BMDM, although IκB levels appeared to recover faster in *Mkp-1*$^{-/-}$ BMDM than in *Mkp-1*$^{+/+}$ BMDM.

Discussion

Previously, we have shown that *Mkp-1*$^{-/-}$ mice exhibited a significantly greater mortality after *E. coli* infection than *Mkp-1*$^{+/+}$ mice (31, 32). The increased mortality is associated with enhanced production of three cytokines: TNF-α, IL-6, and IL-10, elevation of bacterial burden and greater organ damage. Here we showed that in addition to these three cytokines the production of at least another seven cytokines were enhanced in *Mkp-1*$^{-/-}$ mice following systemic *E. coli* infection, including IL-1α and β, IL-17A, IL-27, GM-CSF, IFN-β, and IFN-γ (Fig. 3), highlighting the pivotal role of Mkp-1 in the prevention of cytokine storms. Consistent with the significant increase in circulating IFNs, the expression of a large number of interferon-stimulated genes was substantially enhanced in the livers of *E. coli*-infected *Mkp-1*$^{-/-}$ mice compared to *E. coli*-infected *Mkp-1*$^{+/+}$ mice (Fig. 1). Since the mRNA levels of type I IFNs were very low in livers (Table S2), they are unlikely a major source of type I IFN production during sepsis. We think that the augmented expression of these numerous IFN-stimulated genes in the livers of *E. coli*-infected *Mkp-1*$^{-/-}$ mice is likely a cellular reflection of elevated circulating type I IFNs. In this study, we focus on the function of type I IFN during *E. coli* infection and the regulation of IFN-β expression by Mkp-1. We showed that neutralizing IFNAR1 increased morbidity without affecting TNF-α and IL-6 or bacterial burden, supporting a beneficial role of type I IFNs in this sepsis model (Fig. 4). The expression of Rsad2 protein in *E. coli*-infected *Mkp-1*$^{-/-}$ mice was almost abolished by IFNAR1 neutralization, illustrating the importance of type I IFN signaling in Rsad2 induction and a nearly complete neutralization of type I IFN signaling in these mice (Fig. 4C). Supporting the critical role of Mkp-1 in the regulation of IFN-β production in phagocytes, we found that *Mkp-1*$^{-/-}$ BMDM produced dramatically more IFN-β protein than did *Mkp-1*$^{+/+}$ cells following stimulation with *E. coli*, LPS, poly (I:C), or herring sperm DNA (Figs. 5, 7F). Moreover, enhanced IFN-β induction in response to these agents were almost completely blocked by a p38 inhibitor, but not a JNK inhibitor (Fig. 7), suggesting that enhanced p38 activity is primarily responsible for the increased IFN-β production in *Mkp-1*$^{-/-}$ macrophages. We found that the half-life of *E. coli*-induced IFN-β mRNA was modestly longer in *Mkp-1*$^{-/-}$ BMDM than in *Mkp-1*$^{+/+}$ BMDM (Fig. 8A). We also found that over-expression of Mkp-1 had little effect on the activity of the proximal *IFN-β* promoter (Fig. 8B). *Mkp-1* deficiency had little effect on IRF3 phosphorylation (Fig. 8C), TBK1 or IKKα/β activation (Fig. 8D). Taken together, our results clearly show that Mkp-1 constrains the exaggerated production of many cytokines that are both beneficial and harmful to the host during microbial infections, establishing Mkp-1 as a critical gate keeper of the cytokine storm in sepsis. Our studies indicate that Mkp-1 regulates IFN-β expression primarily through a p38-mediated mechanism.

Mechanisms by which Mkp-1 regulates IFN-β expression

We found that 10 of the 13 cytokines examined in this study exhibited enhanced production following *E. coli* infection in *Mkp-1*$^{-/-}$ mice relative to *Mkp-1*$^{+/+}$ mice (Fig. 3). The exaggerated production of these cytokines in *Mkp-1*$^{-/-}$ mice following *E. coli* infection is not surprising. These are typical inflammatory cytokines and their mRNA transcripts contain adenylate-uridylate (AU)-rich elements in the 3' un-translated regions (64). However, the regulation of IFN-β by Mkp-1 in response to bacterial infection has not been previously

reported. The increased IFN-β production in *E. coli*-infected *Mkp-1*$^{-/-}$ mice and *Mkp-1*$^{-/-}$ BMDM following stimulation with *E. coli*, LPS, poly (I:C), and DNA clearly show an inhibitory role of Mkp-1 in IFN-β induction (Figs. 5, 7). The inhibitory action of Mkp-1 on IFN-β production is further supported by the almost complete suppression of IFN-β production by over-expression of Mkp-1 in *E. coli*- and LPS-stimulated RAW264.7 cells (Fig. 6).

While it is clear that Mkp-1 inhibits IFN-β expression at both the mRNA and protein levels, the mechanism involved is unclear. In theory, Mkp-1 could regulate IFN-β induction through both transcriptional and post-transcriptional mechanisms (65). It has been well-established that *IFN-β* transcription can be regulated by the transcription factors IRF3, IRF7, NF-κB, and AP-1 in a cooperative manner via binding to the positive regulatory domain (PRD) I-IV on the *IFN-β* promoter (62, 63). However, our results suggest that, at least in response to LPS, enhanced IFN-β expression by *Mkp-1* deficiency is unlikely mediated by these transcription factors. *Mkp-1* deficiency did not overtly enhance IRF3 or IRF7 phosphorylation (Fig. 8C) or IKKα/β activity (Fig. 8D). The AP-1 transcription factor complex bound to PRD IV of the *IFN-β* promoter also does not appear to play a prominent role in the enhanced IFN-β expression in *Mkp-1*$^{-/-}$ macrophages, at least in response to LPS. PRD IV-bound AP-1 is composed of a c-Jun/ATF2 heterodimer (63). JNK is known to enhance the transcriptional activity of AP-1 through phosphorylation of c-Jun and ATF2, and p38 also phosphorylates ATF2 (66–69). Mkp-1 deficiency leads to enhanced JNK and p38 activity, which could, at least in theory, enhance AP-1 activity and enhanced *IFN-β* transcription. However, the following observations do not support this model. First, Mkp-1 over-expression in LPS-stimulated RAW264.7 cells had little effect on the activity of the proximal *IFN-β* promoter that contains PRD I-IV (Fig. 8B), although it almost completely inhibited IFN-β production from the endogenous gene after either LPS or *E. coli* stimulation (Figs. 6B, 6C). Second, a JNK-selective inhibitor had little effect on IFN-β expression following LPS stimulation (Figs. 7A, 7B), despite a substantial inhibition of c-Jun phosphorylation (data not shown). The role of AP-1 and JNK in IFN-β expression in response to *E. coli* stimulation appears to be more complicated (Figs. 7A, 8B). This is not surprising, because bacteria are bound to stimulate more signaling pathways due to the increased complexity of the stimulant. JNK appears to play a minor role in *E. coli*-induced IFN-β expression in *Mkp-1*$^{-/-}$ BMDM, since inhibition of both JNK and p38 led to a greater decrease in IFN-β expression than inhibition of p38 alone (Fig. 7A). This limited stimulatory effect of JNK could be mediated by AP-1 transcription factor via PRD IV of the proximal *IFN-β* promoter since *E. coli*-induced *IFN-β*-luciferase reporter activity was modestly inhibited by Mkp-1 over-expression (Fig. 8B). Unlike the limited role of JNK in IFN-β expression, p38 plays a critical role in IFN-β expression for all stimulations tested (Fig. 7). We postulate that if p38 positively regulates *IFN-β* transcription, the action is likely mediated by a transcription factor other than AP-1 through a distal element(s) on the *IFN-β* promoter.

We think that elevated p38 activity in *Mkp-1*$^{-/-}$ macrophages may also mediate IFN-β expression by stabilizing IFN-β mRNA and enhancing IFN-β translation (70). IFN-β mRNA contains several putative AU-rich elements (65, 71, 72). AU-rich elements have been shown to mediate mRNA decay through interaction with mRNA-binding proteins such

as tristetraprolin (TTP) (73). In the absence of Mkp-1, stronger p38 activity could lead to greater TTP phosphorylation, resulting in dissociation of TTP from the IFN-β mRNA decay machinery, leading to enhanced IFN-β mRNA stability and IFN-β translation. This is consistent with our observation that IFN-β mRNA half-life is longer in *Mkp-1*$^{-/-}$ BMDM than in *Mkp-1*$^{+/+}$ BMDM (Fig. 8). Nevertheless, it is still puzzling whether a modest increase in IFN-β mRNA stability could explain the dramatic differences in IFN-β mRNA levels (Fig. 5).

Given the importance of IFN-β in host defense against viruses (41), we speculate that as a negative regulator of IFN-β production Mkp-1 could also be detrimental during certain viral infections, and inhibition of this phosphatase may represent a therapeutic treatment to contain viral spread. This is supported by the substantial enhancement in the expression of the large number of interferon-stimulated genes in the livers of *Mkp-1*$^{-/-}$ mice after *E. coli* infection (Fig. 1). It should be pointed out that IFN-γ likely also contributed to the induction of some of the genes, given the significant differences in IFN-γ levels between the *E. coli*-infected *Mkp-1*$^{+/+}$ and *Mkp-1*$^{-/-}$ mice (Fig. 3).

IFN-β and the phenotype of Mkp-1$^{-/-}$ mice during E. coli sepsis

Mkp-1$^{-/-}$ mice exhibit enhanced cytokine production, elevated bacterial burden, and increased mortality following systemic *E. coli* infection relative to *Mkp-1*$^{+/+}$ mice (31). Since IFN-β has been shown to play both beneficial and detrimental roles during bacterial infection (33, 74), we blocked the receptor for IFN-β, IFNAR1, and examined the effects on both mortality and morbidity after *E. coli* infection. Complete blockade of type I IFN signaling by the IFNAR1-neutralizing antibody was supported by the absence of Rsad2 protein (Fig. 4C), a classic IFN-stimulated gene (75). Neutralizing IFNAR1 not only led to significantly greater disease severity but also appeared to increase the mortality in *Mkp-1*$^{-/-}$ mice (Figs. 4A, 4B). These results suggest that elevated IFN-β is beneficial to the animals in this sepsis model but how this occurs is unclear. Neutralizing IFN-β neither altered IL-6 production, an inflammatory index, nor changed bacterial burden (Figs. 4C, 4D). IFN-β has been shown to influence the immune system through a number of processes and systems, including tissue and cell integrity, and barrier functions (74, 76). Regardless of the exact mechanism via which IFN-β influences the host response in our *E. coli*-induced sepsis model, it is clear that elevated IFN-β production is not responsible for the elevated bacterial burden and increased mortality of *Mkp-1*$^{-/-}$ mice.

Supplementary Material

Refer to Web version on PubMed Central for supplementary material.

Acknowledgments

We are grateful to Bristol-Myers Squibb Pharmaceutical Research Institute for proving Mkp-1 knockout mice. We thank Drs. Xianxi Wang, Jinhui Li, Xiaomei Meng, and Dimitrios Anastasakis for help with in vivo infection and RNA-seq experiments. We also gratefully acknowledge William M. White for technical support. We thank Dr. Yongliang Zhang for generously providing the *IFN-β*-luciferase reporter and thank Dr. Stefanie Vogel for valuable suggestions.

This work was supported by grants from NIH (AI124029 and AI142885 and to Y.L., and AI121196 to J.Z.).

Abbreviations used:

3

ATF2	activating transcription factor 2
AU	adenylate-uridylate
BMDM	bone marrow-derived macrophages
b.w.	body weight
cGAS	cyclic AMP-GMP synthase
Dox	doxycycline
Fasn	fatty acid synthase
IFN	interferon
IFNAR1	IFN-α/β receptor 1
IKK	IκB kinase
IRF	interferon regulatory factor
Isg	interferon-stimulated gene
JNK-IN-8	JNK inhibitor 8
Mkp-1	MAP kinase phosphatase-1
Mx	myxovirus resistance
Nampt	nicotinamide phosphoribosyltransferase
Oasl1	2’−5’-oligoadenylate synthase-like protein 1
poly (I:C)	polyinosinic:polycytidylic acid
PRD	positive regulatory domain
qRT-PCR	quantitative RT-PCR
Rsad2	radical S-adenosyl methionine domain containing protein 2
STING	stimulator of interferon genes
TTP	tristetraprolin
TBK1	TANK-binding kinase 1
Usp 18	ubiquitin specific peptidase 18

References

1. Janeway CA Jr., Travers P, Walport M, and Shlomchik MJ. 2001. Immunobiology: the immune system in health and disease. Garland Publishing, New York.
2. Medzhitov R, and Janeway C Jr. 2000. The Toll receptor family and microbial recognition. Trends Microbiol 8: 452–456. [PubMed: 11044679]
3. Akira S 2003. Mammalian Toll-like receptors. Curr. Opin. Immunol 15: 5–11. [PubMed: 12495726]
4. Cook DN, Pisetsky DS, and Schwartz DA. 2004. Toll-like receptors in the pathogenesis of human disease. Nat.Immunol 5: 975–979. [PubMed: 15454920]
5. Kaisho T, and Akira S. 2000. Critical roles of Toll-like receptors in host defense. Crit Rev.Immunol 20: 393–405. [PubMed: 11145217]
6. Takeuchi O, and Akira S. 2001. Toll-like receptors; their physiological role and signal transduction system. Int.Immunopharmacol 1: 625–635. [PubMed: 11357875]
7. Hawiger J 2001. Innate immunity and inflammation: a transcriptional paradigm. Immunol. Res 23: 99–109. [PubMed: 11444396]
8. Dong C, Davis RJ, and Flavell RA. 2002. MAP kinases in the immune response. Annu. Rev. Immunol 20: 55–72. [PubMed: 11861597]
9. Hayden MS, West AP, and Ghosh S. 2006. NF-kappaB and the immune response. Oncogene 25: 6758–6780. [PubMed: 17072327]
10. Kafka D, Ling E, Feldman G, Benharroch D, Voronov E, Givon-Lavi N, Iwakura Y, Dagan R, Apte RN, and Mizrachi-Nebenzahl Y. 2008. Contribution of IL-1 to resistance to Streptococcus pneumoniae infection. Int Immunol 20: 1139–1146. [PubMed: 18596024]
11. Prantner D, Darville T, Sikes JD, Andrews CW Jr., Brade H, Rank RG, and Nagarajan UM. 2009. Critical role for interleukin-1beta (IL-1beta) during Chlamydia muridarum genital infection and bacterial replication-independent secretion of IL-1beta in mouse macrophages. Infect Immun 77: 5334–5346. [PubMed: 19805535]
12. Conti HR, and Gaffen SL. 2015. IL-17-Mediated Immunity to the Opportunistic Fungal Pathogen Candida albicans. J. Immunol 195: 780–788. [PubMed: 26188072]
13. Dalrymple SA, Lucian LA, Slattery R, McNeil T, Aud DM, Fuchino S, Lee F, and Murray R. 1995. Interleukin-6-deficient mice are highly susceptible to Listeria monocytogenes infection: correlation with inefficient neutrophilia. Infect. Immun 63: 2262–2268. [PubMed: 7768607]
14. Beutler B 1995. TNF, immunity and inflammatory disease: lessons of the past decade. J. Investig. Med 43: 227–235.
15. Peñaloza HF, Nieto PA, Muñoz-Durango N, Salazar-Echegarai FJ, Torres J, Parga MJ, Alvarez-Lobos M, Riedel CA, Kalergis AM, and Bueno SM. 2015. Interleukin-10 plays a key role in the modulation of neutrophils recruitment and lung inflammation during infection by Streptococcus pneumoniae. Immunology 146: 100–112. [PubMed: 26032199]
16. Keyse SM 1998. Protein phosphatases and the regulation of MAP kinase activity. Semin. Cell Dev. Biol 9: 143–152. [PubMed: 9599409]
17. Keyse SM, and Emslie EA. 1992. Oxidative stress and heat shock induce a human gene encoding a protein-tyrosine phosphatase. Nature 359: 644–647. [PubMed: 1406996]
18. Charles CH, Sun H, Lau LF, and Tonks NK. 1993. The growth factor-inducible immediate-early gene 3CH134 encodes a protein-tyrosine-phosphatase. Proc Natl Acad Sci U S A 90: 5292–5296. [PubMed: 8389479]
19. Noguchi T, Metz R, Chen L, Mattei MG, Carrasco D, and Bravo R. 1993. Structure, mapping, and expression of erp, a growth factor-inducible gene encoding a nontransmembrane protein tyrosine phosphatase, and effect of ERP on cell growth. Mol. Cell Biol 13: 5195–5205. [PubMed: 8355678]
20. Keyse SM 2000. Protein phosphatases and the regulation of mitogen-activated protein kinase signalling. Curr. Opin. Cell Biol 12: 186–192. [PubMed: 10712927]
21. Franklin CC, and Kraft AS. 1997. Conditional expression of the mitogen-activated protein kinase (MAPK) phosphatase MKP-1 preferentially inhibits p38 MAPK and stress-activated protein kinase in U937 cells. J. Biol. Chem 272: 16917–16923. [PubMed: 9202001]

22. Liu Y, Shepherd EG, and Nelin LD. 2007. MAPK phosphatases - regulating the immune response. Nat. Rev. Immunol 7: 202–212. [PubMed: 17318231]

23. Lang R, Hammer M, and Mages J. 2006. DUSP meet immunology: dual specificity MAPK phosphatases in control of the inflammatory response. J. Immunol 177: 7497–7504. [PubMed: 17114416]

24. Shepherd EG, Zhao Q, Welty SE, Hansen TN, Smith CV, and Liu Y. 2004. The function of mitogen-activated protein kinase phosphatase-1 in peptidoglycan-stimulated macrophages. J Biol Chem 279: 54023–54031. [PubMed: 15485842]

25. Zhao Q, Shepherd EG, Manson ME, Nelin LD, Sorokin A, and Liu Y. 2005. The role of mitogen-activated protein kinase phosphatase-1 in the response of alveolar macrophages to lipopolysaccharide: Attenuation of proinflammatory cytokine biosynthesis via feedback control of p38. J. Biol. Chem 280: 8101–8108. [PubMed: 15590669]

26. Zhao Q, Wang X, Nelin LD, Yao Y, Matta R, Manson ME, Baliga RS, Meng X, Smith CV, Bauer JA, Chang CH, and Liu Y. 2006. MAP kinase phosphatase 1 controls innate immune responses and suppresses endotoxic shock. J. Exp. Med 203: 131–140. [PubMed: 16380513]

27. Hammer M, Mages J, Dietrich H, Servatius A, Howells N, Cato AC, and Lang R. 2006. Dual specificity phosphatase 1 (DUSP1) regulates a subset of LPS-induced genes and protects mice from lethal endotoxin shock. J. Exp. Med 203: 15–20. [PubMed: 16380512]

28. Chi H, Barry SP, Roth RJ, Wu JJ, Jones EA, Bennett AM, and Flavell RA. 2006. Dynamic regulation of pro- and anti-inflammatory cytokines by MAPK phosphatase 1 (MKP-1) in innate immune responses. Proc. Natl. Acad. Sci U. S. A 103: 2274–2279. [PubMed: 16461893]

29. Salojin KV, Owusu IB, Millerchip KA, Potter M, Platt KA, and Oravecz T. 2006. Essential role of MAPK phosphatase-1 in the negative control of innate immune responses. J. Immunol 176: 1899–1907. [PubMed: 16424221]

30. Manetsch M, Che W, Seidel P, Chen Y, and Ammit AJ. 2012. MKP-1: a negative feedback effector that represses MAPK-mediated pro-inflammatory signaling pathways and cytokine secretion in human airway smooth muscle cells. Cell Signal 24: 907–913. [PubMed: 22200679]

31. Frazier WJ, Wang X, Wancket LM, Li XA, Meng X, Nelin LD, Cato AC, and Liu Y. 2009. Increased inflammation, impaired bacterial clearance, and metabolic disruption after gram-negative sepsis in Mkp-1-deficient mice. J. Immunol 183: 7411–7419. [PubMed: 19890037]

32. Li J, Wang X, Ackerman WE, Batty AJ, Kirk SG, White WM, Wang X, Anastasakis D, Samavati L, Buhimschi I, Nelin LD, Hafner M, and Liu Y. 2018. Dysregulation of Lipid Metabolism in Mkp-1 Deficient Mice during Gram-Negative Sepsis. Int. J. Mol. Sci 19: 3904.

33. Bogdan C 2000. The function of type I interferons in antimicrobial immunity. Curr Opin Immunol 12: 419–424. [PubMed: 10899033]

34. Patel JR, and García-Sastre A. 2014. Activation and regulation of pathogen sensor RIG-I. Cytokine Growth Factor Rev 25: 513–523. [PubMed: 25212896]

35. Zuniga EI, Hahm B, and Oldstone MB. 2007. Type I interferon during viral infections: multiple triggers for a multifunctional mediator. Curr Top Microbiol Immunol 316: 337–357. [PubMed: 17969455]

36. Hemmi H, Takeuchi O, Sato S, Yamamoto M, Kaisho T, Sanjo H, Kawai T, Hoshino K, Takeda K, and Akira S. 2004. The roles of two IkappaB kinase-related kinases in lipopolysaccharide and double stranded RNA signaling and viral infection. J. Exp. Med 199: 1641–1650. [PubMed: 15210742]

37. McWhirter SM, Fitzgerald KA, Rosains J, Rowe DC, Golenbock DT, and Maniatis T. 2004. IFN-regulatory factor 3-dependent gene expression is defective in Tbk1-deficient mouse embryonic fibroblasts. Proc. Natl. Acad. Sci. U. S. A 101: 233–238. [PubMed: 14679297]

38. Perry AK, Chow EK, Goodnough JB, Yeh WC, and Cheng G. 2004. Differential requirement for TANK-binding kinase-1 in type I interferon responses to toll-like receptor activation and viral infection. J. Exp. Med 199: 1651–1658. [PubMed: 15210743]

39. Scumpia PO, Botten GA, Norman JS, Kelly-Scumpia KM, Spreafico R, Ruccia AR, Purbey PK, Thomas BJ, Modlin RL, and Smale ST. 2017. Opposing roles of Toll-like receptor and cytosolic DNA-STING signaling pathways for Staphylococcus aureus cutaneous host defense. PLoS. Pathog 13: e1006496. [PubMed: 28704551]

40. Zevini A, Olagnier D, and Hiscott J. 2017. Crosstalk between Cytoplasmic RIG-I and STING Sensing Pathways. Trends Immunol 38: 194–205. [PubMed: 28073693]
41. McNab F, Mayer-Barber K, Sher A, Wack A, and O'Garra A. 2015. Type I interferons in infectious disease. Nat Rev Immunol 15: 87–103. [PubMed: 25614319]
42. Trinchieri G 2010. Type I interferon: friend or foe? J Exp Med 207: 2053–2063. [PubMed: 20837696]
43. Boxx GM, and Cheng G. 2016. The Roles of Type I Interferon in Bacterial Infection. Cell Host Microbe 19: 760–769. [PubMed: 27281568]
44. Dorfman K, Carrasco D, Gruda M, Ryan C, Lira SA, and Bravo R. 1996. Disruption of the erp/mkp-1 gene does not affect mouse development: normal MAP kinase activity in ERP/MKP-1-deficient fibroblasts. Oncogene 13: 925–931. [PubMed: 8806681]
45. Shrum B, Anantha RV, Xu SX, Donnelly M, Haeryfar SM, McCormick JK, and Mele T. 2014. A robust scoring system to evaluate sepsis severity in an animal model. BMC Res Notes 7: 233. [PubMed: 24725742]
46. Konstantinou GN 2017. Enzyme-Linked Immunosorbent Assay (ELISA). Methods Mol Biol 1592: 79–94. [PubMed: 28315213]
47. Zhao Q, Chen P, Manson ME, and Liu Y. 2006. Production of active recombinant mitogen-activated protein kinases through transient transfection of 293T cells. Protein Expr. Purif 46: 468–474. [PubMed: 16256366]
48. Lee JC, Laydon JT, McDonnell PC, Gallagher TF, Kumar S, Green D, McNulty D, Blumenthal MJ, Heys JR, and Landvatter SW. 1994. A protein kinase involved in the regulation of inflammatory cytokine biosynthesis. Nature 372: 739–746. [PubMed: 7997261]
49. Zhang T, Inesta-Vaquera F, Niepel M, Zhang J, Ficarro SB, Machleidt T, Xie T, Marto JA, Kim N, Sim T, Laughlin JD, Park H, LoGrasso PV, Patricelli M, Nomanbhoy TK, Sorger PK, Alessi DR, and Gray NS. 2012. Discovery of potent and selective covalent inhibitors of JNK. Chem. Biol 19: 140–154. [PubMed: 22284361]
50. Kim VY, Batty A, Li J, Kirk SG, Crowell SA, Jin Y, Tang J, Zhang J, Rogers LK, Deng HX, Nelin LD, and Liu Y. 2019. Glutathione Reductase Promotes Fungal Clearance and Suppresses Inflammation during Systemic Candida albicans Infection in Mice. J. Immunol 203: 2239–2251. [PubMed: 31501257]
51. Yusa K, Zhou L, Li MA, Bradley A, and Craig NL. 2011. A hyperactive piggyBac transposase for mammalian applications. Proc Natl Acad Sci U S A 108: 1531–1536. [PubMed: 21205896]
52. Cortazar MA, Sheridan RM, Erickson B, Fong N, Glover-Cutter K, Brannan K, and Bentley DL. 2019. Control of RNA Pol II Speed by PNUTS-PP1 and Spt5 Dephosphorylation Facilitates Termination by a "Sitting Duck Torpedo" Mechanism. Mol Cell 76: 896–908 e894. [PubMed: 31677974]
53. Barger CJ, Branick C, Chee L, and Karpf AR. 2019. Pan-Cancer Analyses Reveal Genomic Features of FOXM1 Overexpression in Cancer. Cancers (Basel) 11: 251 doi: 210.3390/cancers11020251.
54. Rocha BC, Marques PE, Leoratti FMS, Junqueira C, Pereira DB, Antonelli L, Menezes GB, Golenbock DT, and Gazzinelli RT. 2015. Type I interferon transcriptional signature in neutrophils and low-density granulocytes are associated with tissue damage in malaria. Cell Rep 13: 2829–2841. [PubMed: 26711347]
55. Chen P, Li J, Barnes J, Kokkonen GC, Lee JC, and Liu Y. 2002. Restraint of proinflammatory cytokine biosynthesis by mitogen-activated protein kinase phosphatase-1 in lipopolysaccharide-stimulated macrophages. J. Immunol 169: 6408–6416. [PubMed: 12444149]
56. Yamamoto M, Sato S, Hemmi H, Hoshino K, Kaisho T, Sanjo H, Takeuchi O, Sugiyama M, Okabe M, Takeda K, and Akira S. 2003. Role of adaptor TRIF in the MyD88-independent toll-like receptor signaling pathway. Science 301: 640–643. [PubMed: 12855817]
57. Schmitz F, Mages J, Heit A, Lang R, and Wagner H. 2004. Transcriptional activation induced in macrophages by Toll-like receptor (TLR) ligands: from expression profiling to a model of TLR signaling. Eur J Immunol 34: 2863–2873. [PubMed: 15368303]
58. Beutler B 2000. Tlr4: central component of the sole mammalian LPS sensor. Curr. Opin. Immunol 12: 20–26. [PubMed: 10679411]

59. Alexopoulou L, Holt AC, Medzhitov R, and Flavell RA. 2001. Recognition of double-stranded RNA and activation of NF-kappaB by Toll-like receptor 3. Nature 413: 732–738. [PubMed: 11607032]
60. Kumar H, Kawai T, and Akira S. 2011. Pathogen recognition by the innate immune system. Int. Rev. Immunol 30: 16–34. [PubMed: 21235323]
61. Bode C, Fox M, Tewary P, Steinhagen A, Ellerkmann RK, Klinman D, Baumgarten G, Hornung V, and Steinhagen F. 2016. Human plasmacytoid dentritic cells elicit a Type I Interferon response by sensing DNA via the cGAS-STING signaling pathway. Eur J Immunol 46: 1615–1621. [PubMed: 27125983]
62. Pålsson-McDermott EM, and O'Neill LA. 2004. Signal transduction by the lipopolysaccharide receptor, Toll-like receptor-4. Immunology 113: 153–162. [PubMed: 15379975]
63. Honda K, Takaoka A, and Taniguchi T. 2006. Type I interferon [corrected] gene induction by the interferon regulatory factor family of transcription factors. Immunity 25: 349–360. [PubMed: 16979567]
64. Clark A, Dean J, Tudor C, and Saklatvala J. 2009. Post-transcriptional gene regulation by MAP kinases via AU-rich elements. Front Biosci. (Landmark. Ed) 14: 847–871. [PubMed: 19273104]
65. McGuire VA, Rosner D, Ananieva O, Ross EA, Elcombe SE, Naqvi S, van den Bosch MMW, Monk CE, Ruiz-Zorrilla Diez T, Clark AR, and Arthur JSC. 2017. Beta Interferon Production Is Regulated by p38 Mitogen-Activated Protein Kinase in Macrophages via both MSK1/2- and Tristetraprolin-Dependent Pathways. Mol Cell Biol 37.
66. Karin M 1995. The regulation of AP-1 activity by mitogen-activated protein kinases. J. Biol. Chem 270: 16483–16486. [PubMed: 7622446]
67. Davis RJ 1995. Transcriptional regulation by MAP kinases. Mol. Reprod. Dev 42: 459–467. [PubMed: 8607977]
68. Gupta S, Campbell D, Derijard B, and Davis RJ. 1995. Transcription factor ATF2 regulation by the JNK signal transduction pathway. Science 267: 389–393. [PubMed: 7824938]
69. Derijard B, Hibi M, Wu IH, Barrett T, Su B, Deng T, Karin M, and Davis RJ. 1994. JNK1: a protein kinase stimulated by UV light and Ha-Ras that binds and phosphorylates the c-Jun activation domain. Cell 76: 1025–1037. [PubMed: 8137421]
70. O'Neil JD, Ammit AJ, and Clark AR. 2018. MAPK p38 regulates inflammatory gene expression via tristetraprolin: Doing good by stealth. Int. J. Biochem. Cell Biol 94:6–9. doi: 10.1016/j.biocel.2017.11.003. Epub; 2017 Nov 8.: 6–9. [PubMed: 29128684]
71. Lin WJ, Zheng X, Lin CC, Tsao J, Zhu X, Cody JJ, Coleman JM, Gherzi R, Luo M, Townes TM, Parker JN, and Chen CY. 2011. Posttranscriptional control of type I interferon genes by KSRP in the innate immune response against viral infection. Mol Cell Biol 31: 3196–3207. [PubMed: 21690298]
72. Pasté M, Huez G, and Kruys V. 2003. Deadenylation of interferon-beta mRNA is mediated by both the AU-rich element in the 3'-untranslated region and an instability sequence in the coding region. Eur J Biochem 270: 1590–1597. [PubMed: 12654014]
73. Rigby WF, Roy K, Collins J, Rigby S, Connolly JE, Bloch DB, and Brooks SA. 2005. Structure/function analysis of tristetraprolin (TTP): p38 stress-activated protein kinase and lipopolysaccharide stimulation do not alter TTP function. J. Immunol 174: 7883–7893. [PubMed: 15944294]
74. Boxx GM, and Cheng G. 2016. The Roles of Type I Interferon in Bacterial Infection. Cell Host. Microbe 19: 760–769. [PubMed: 27281568]
75. Nasr N, Maddocks S, Turville SG, Harman AN, Woolger N, Helbig KJ, Wilkinson J, Bye CR, Wright TK, Rambukwelle D, Donaghy H, Beard MR, and Cunningham AL. 2012. HIV-1 infection of human macrophages directly induces viperin which inhibits viral production. Blood 120: 778–788. [PubMed: 22677126]
76. Kovarik P, Castiglia V, Ivin M, and Ebner F. 2016. Type I Interferons in Bacterial Infections: A Balancing Act. Front Immunol 7:652. doi: 10.3389/fimmu.2016.00652. [PubMed: 28082986]

Key points

- Knockout of Mkp-1 exacerbates cytokine storms during *E. coli*-induced sepsis.
- Mkp-1 restrains IFN-β expression in macrophages by controlling p38 activity.
- Blocking type I IFN signaling during *E. coli* infection exacerbate disease severity.

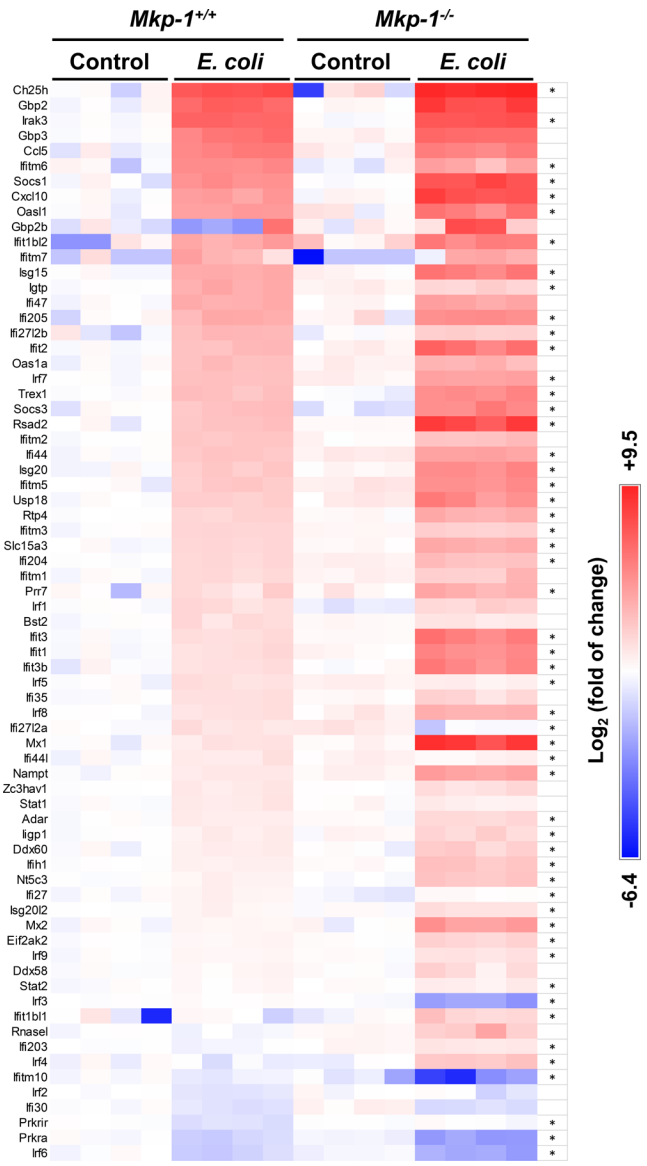

Figure 1. *Mkp-1* deficiency dramatically enhanced hepatic expression of interferon-responsive genes in *E. coli*-infected mice.

Mkp-1$^{-/-}$ and *Mkp-1*$^{+/+}$ mice on a C57/129 background were infected i.v. with live *E. coli* at a dose of 2.5×10^7 CFU/g b.w. or injected with PBS (controls). Mice were euthanized after 24 h, and total RNA was isolated from the livers using Trizol for RNA-seq analyses. The copy numbers of RNA transcripts for each interferon-responsive gene were normalized to the average number in wildtype controls to calculate fold change. The interferon-responsive genes were ranked based on the fold change in RNA transcripts in wildtype mice following *E. coli* infection. These values were $\log_2$-transformed to generate the heat map. Log-transformation allows for a greater scale in the heat map. When the transcript number is 0 for a given gene in a specific animal, we gave an arbitrary number that is lower than the lowest value in that group. Each column represents a distinct animal. *, $p<0.05$, comparing *E. coli*-infected *Mkp-1*$^{-/-}$ and *E. coli*-infected *Mkp-1*$^{+/+}$ mice (t-test, n=4).

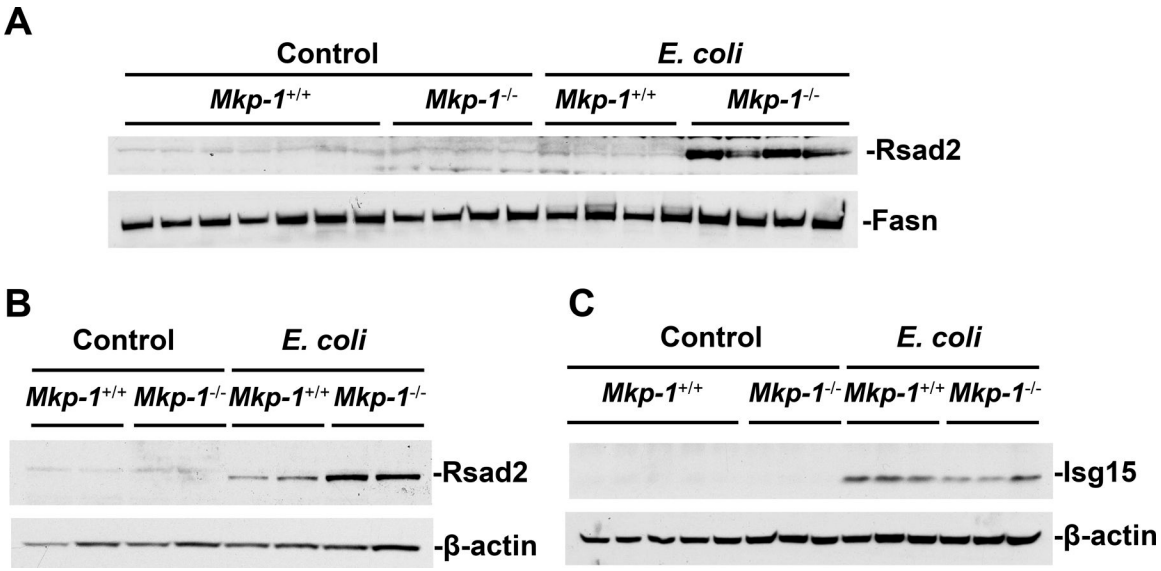

Figure 2. Increased Rsad2 protein expression and serum IFN-β production in *Mkp-1*$^{-/-}$ mice relative to *Mkp-1*$^{+/+}$ mice following *E. coli* infection.

Mkp-1$^{-/-}$ and *Mkp-1*$^{+/+}$ mice on a C57/129 background were infected i.v. with live *E. coli* at a dose of 2.5 × 10^7 CFU/g b.w. or injected with PBS (controls). Mice were euthanized after 24 h to harvest blood and liver. Serum samples were used for measuring IFN-β by ELISA. Liver tissues were homogenized to extract protein for Western blot analysis using Rsad2 or Isg15 antibody. **A.** Levels of Rsad2 proteins in the livers of control and *E. coli*-infected mice. Each lane represents a different animal. The same set of samples was also analyzed by Western blotting using a mouse monoclonal antibody against a house-keeping protein, fatty acid synthase (Fasn), to verify comparable loading (Lower panel). Liver Rsad2 (**B**) and Isg15 (**C**) protein levels in control and *E. coli*-infected *Mkp-1*$^{-/-}$ and *Mkp-1*$^{+/+}$ mice. Same membranes were stripped and reprobed with a β-actin antibody. Images shown in B and C are representative Western blotting results.

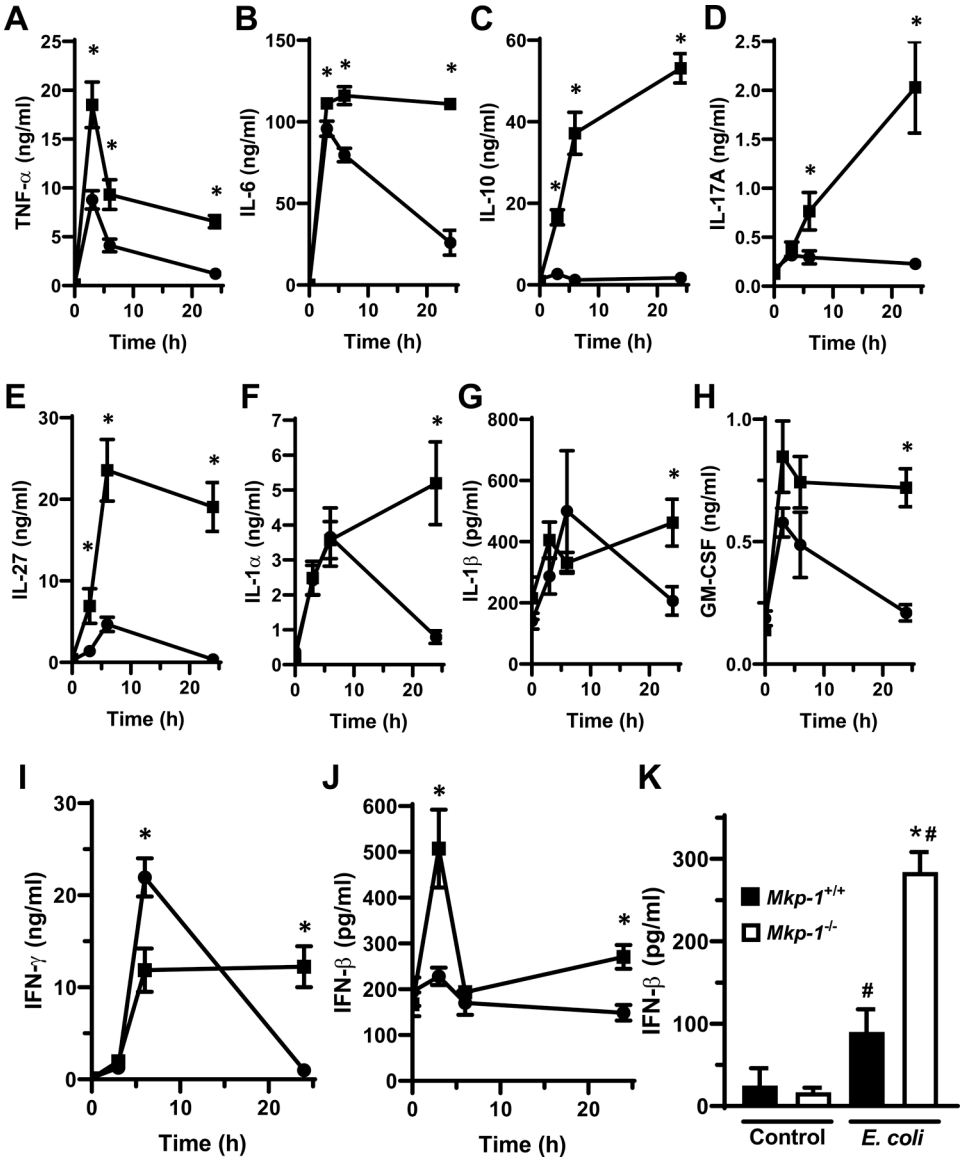

Figure 3. *Mkp-1* deficiency resulted in greater serum cytokine levels in *E. coli*-infected mice.

Mkp-1$^{-/-}$ and *Mkp-1*$^{+/+}$ mice on a C57/129 background were infected i.v. with live *E. coli* at a dose of 2.5 × 10^7 CFU/g body weight or left uninfected. Mice were euthanized at 3, 6, and 24 h post infection (n=8 for all groups). Uninfected mice (n=10 for both groups) were also euthanized and regarded as 0 time point. The blood was collected through cardiac puncture, and serum cytokine levels were measured using a LEGENDplex inflammation kit (**A-I**) to quantify 13 pre-defined mouse cytokines. Cytokine levels are presented as mean ± S.E. in the graphs. Only cytokines that displayed significant differences between the two groups of mice are presented in the graphs. ● represents *Mkp-1*$^{+/+}$ group while ■ represents *Mkp-1*$^{-/-}$ group. **A.** TNF-α; **B.** IL-6; **C.** IL-10; **D.** IL-17A; **E.** IL-27; **F.** IL-1α; **G.** IL-1β; **H.** GM-CSF; **I.** IFN-γ; **J.** IFN-β; **K.** Serum IFN-β concentration measured by ELISA. *, p<0.05, compared to cytokine levels in *E. coli*-infected *Mkp-1*$^{+/+}$ mice at the

same time-point (t-test, n=5–10). #, $p<0.05$, compared to control of the same phenotype (t-test, n=3–10).

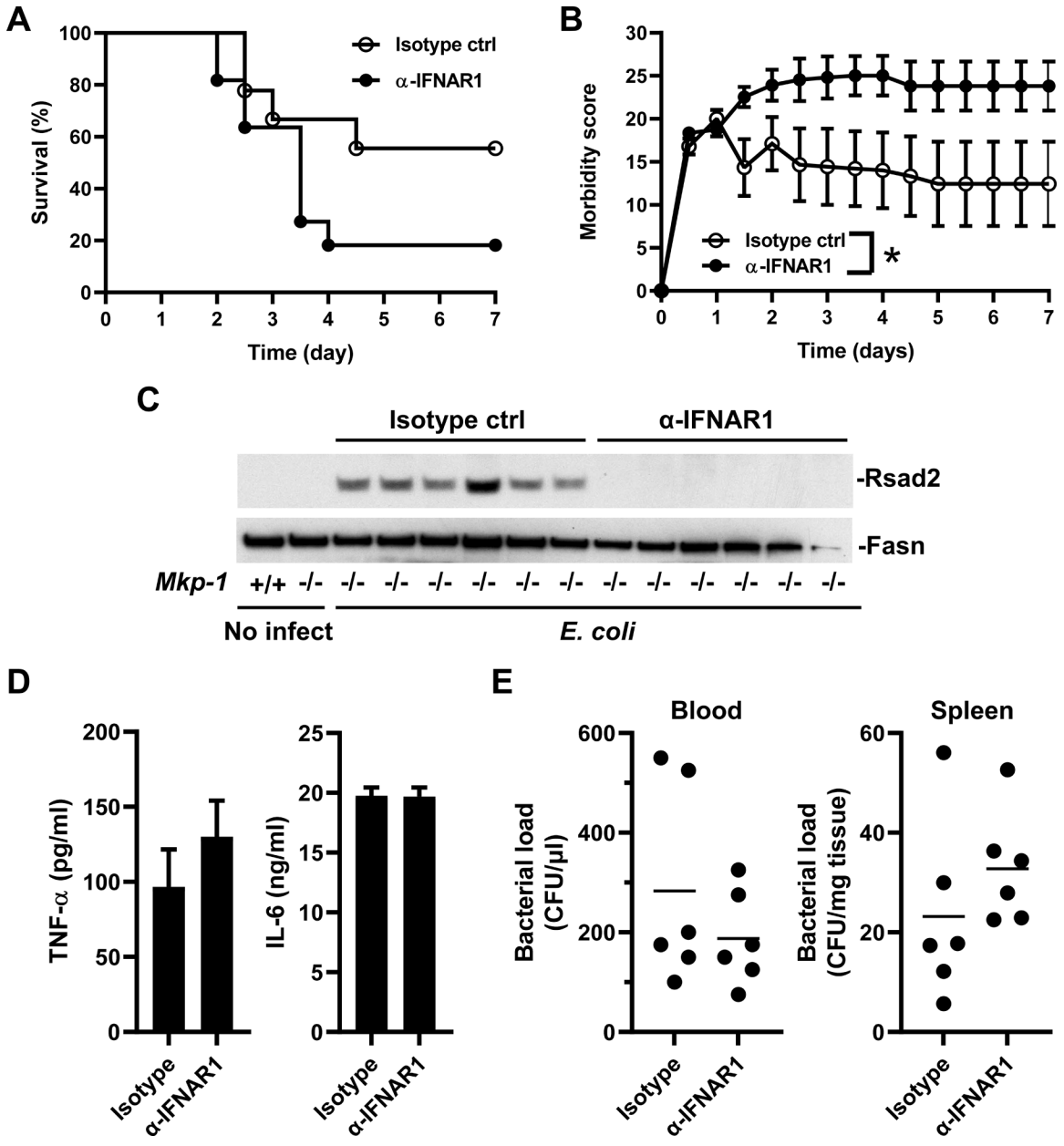

Figure 4. Neutralizing IFN-β exacerbated the severity of disease in *E coli*-infected *Mkp-1*$^{-/-}$ mice.

Mkp-1$^{-/-}$ mice of the C57/129 background were given i.p. 100 μg (per mouse) of either a monoclonal anti-mouse IFNAR1 or an isotype control (IgG1) antibody 1 h prior to *E. coli* infection. These mice were subsequently infected i.v. with live *E. coli* (O55:B5) at a dose of 3.2×10^6 CFU/g body weight. Mice were monitored for 7 days to evaluate mortality and morbidity. To assess IFNAR1 neutralization on liver protein levels, blood cytokines, and bacterial burdens, mice were sacrificed 24 h post *E. coli* infection. Livers, blood, and spleens were collected aseptically. **A.** Survival curves of the *Mkp-1*$^{-/-}$ mice receiving either the isotype control or the anti-IFNAR1 antibody. **B.** Morbidity scores for the *Mkp-1*$^{-/-}$ mice receiving either the isotype control or the anti-IFNAR1 antibody.

The morbidity scores increased over time in both groups and were significantly greater in the group that got anti-IFNAR1 antibody than in the group that got isotype control. By two-way ANOVA the morbidity scores were significantly different for both the group ($p<0.05$) and time ($p<0.001$), and there was a significant interaction between group and time, $p<0.001$. In Panels A and B: $n_{\text{isotype ctrl}}=9$; $n_{\text{IFNAR1}}=11$. **C.** IFNAR-1 neutralizing antibody blocks Rsad2 induction in *E. coli*-infected mice. Livers were homogenized to extract soluble proteins for Western blot analysis using a monoclonal antibody against Rsad2. The membrane was stripped and blotted with a monoclonal antibody against Fasn. **D.** Serum TNF-α and IL-6 levels. Serum TNF-α and IL-6 levels were measured by ELISA. Results represent the means ± SE (n=6). **E.** Bacterial burdens. Bacterial load in the blood and spleen homogenates were determined by culture. Each dot represents an individual animal. Horizontal line represents mean value of CFU.

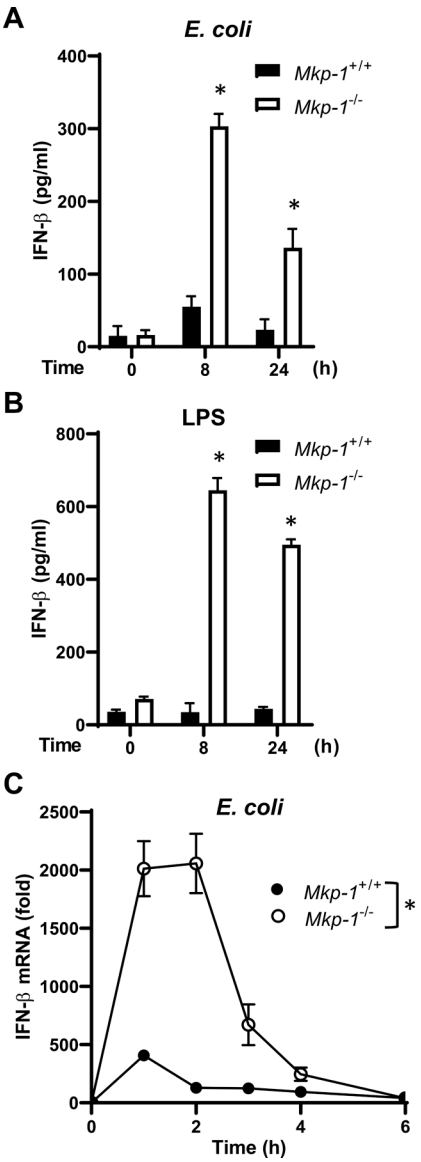

Figure 5. *Mkp-1*-deficient BMDM produced significantly more IFN-β than did wildtype BMDM after LPS and *E. coli* stimulation.

BMDM derived from *Mkp-1*$^{-/-}$ and *Mkp-1*$^{+/+}$ mice of a C57BL/6J background were treated with heat-killed *E. coli* at a dose of 10 bacteria per macrophage or 100 ng/ml LPS (O55:B5). Medium was harvested at different time-points to measure IFN-β concentration by ELISA. Total RNA was isolated from the cells to assess IFN-β mRNA levels by qRT-PCR. **A.** IFN-β production by *Mkp-1*$^{-/-}$ and *Mkp-1*$^{+/+}$ macrophages following *E. coli* stimulation. Values represent mean ± SE (n=4). *, p<0.05, compared to *Mkp-1*$^{+/+}$ macrophages at the same time point (t-test). **B.** IFN-β production by *Mkp-1*$^{-/-}$ and *Mkp-1*$^{+/+}$ macrophages following LPS stimulation (t-test). Values represent mean ± SE (n=4). *, p<0.05, compared to *Mkp-1*$^{+/+}$ macrophages at the same time point (t-test). **C.** Kinetics of IFN-β mRNA levels in macrophages stimulated with heat-killed *E. coli*. IFN-β mRNA expression was presented as fold of change relative to the control cells. Values represent mean ± SE (n=3). IFN-β mRNA significantly changed over time in both genotypes and those changes were

significantly greater in the *Mkp-1*$^{-/-}$ mice than in the *Mkp-1*$^{+/+}$ mice. By two-way ANOVA both time and genotype were significantly different, $p<0.001$ and there was an interaction between genotype and time, $p<0.001$.

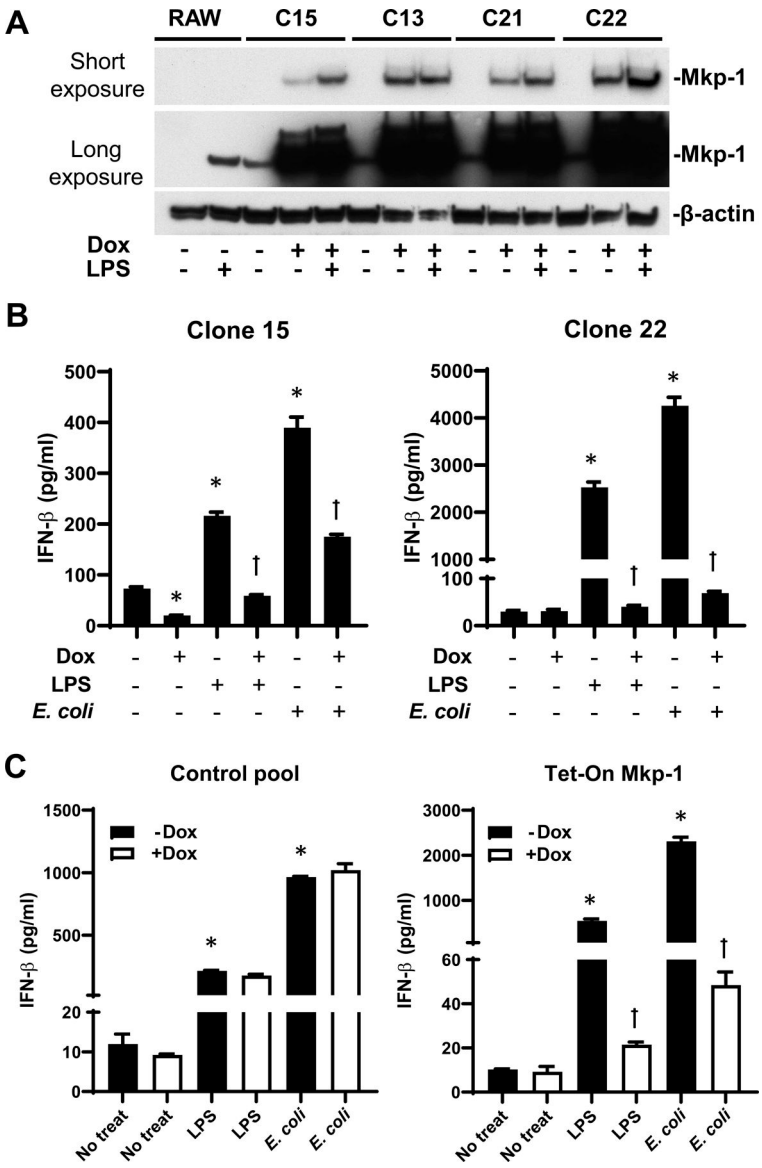

Figure 6. Over-expression of Mkp-1 potently inhibited IFN-β production in LPS-stimulated RAW264.7 macrophages.

RAW264.7 cells were stably transfected with a Tet-ON expression cassette to express a rat Mkp-1 protein. Stable clones represent individual colonies after drug selection. **A.** Expression of Mkp-1 in different clones after treatment with or without LPS in the absence or presence of doxycycline (Dox). RAW264.7 cells or individual clones were pretreated with or without 500 ng/ml doxycycline overnight, and the stimulated with or without LPS (100 ng/ml) for 1 h. Cells were harvested for Western blot analysis. Upper panel represents a short exposure, and the lower panel is a longer exposure to show induction of endogenous Mkp-1 by LPS. **B.** Inhibition of IFN-β production by doxycycline-induced Mkp-1. Cells (10^6) of clone 15 and clone 22 were cultured on 24 well plates in 1 ml medium containing 0 or 100 ng/ml doxycycline overnight, and then stimulated with 100 ng/ml LPS or heat-killed *E. coli* at a dose of 10 bacteria per macrophage for 6 h. Media were harvested for ELISA. Values represent mean ± SE (n=4). *, $p<0.05$, compared to untreated cells. †, $p<0.05$,

compared to cells treated with LPS or *E. coli* in the absence of doxycycline. **C.** The effect of doxycycline pretreatment on IFN-β production in control and Tet-ON Mkp-1-expressing pool. RAW264.7 pools stably transfected with a Tet-ON Mkp-1 expression cassette (Tet-ON-Mkp-1 pool) or an empty vector (Control pool) were first pre-treated with 0 or 100 ng/ml doxycycline overnight, and then stimulated with 100 ng/ml LPS or heat-killed *E. coli* at a dose of 10 bacteria per macrophage for 6 h. *, $p<0.05$, compared to cells that received no doxycycline pre-treatment (- Dox) and were not treated by either LPS or *E. coli*. Values were compared between groups by t-test.

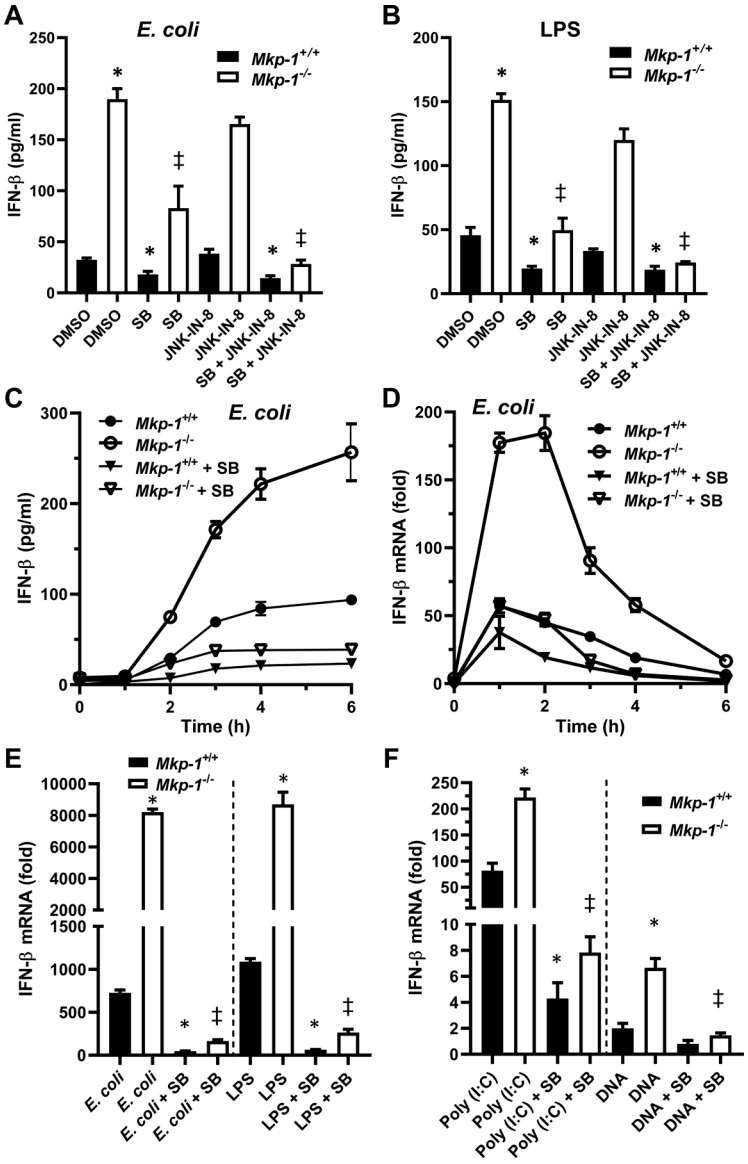

Figure 7. Enhanced IFN-β induction by *E. coli* and TLR ligands caused by Mkp-1 deficiency is substantially inhibited by the pharmacological inhibitor of p38 but not JNK.

Mkp-1$^{-/-}$ and *Mkp-1*$^{+/+}$ BMDM were pre-treated with DMSO (vehicle) or 10 μM SB203580 or 3 μM JNK-IN-8 for 30 min, and then stimulated with heat-killed *E. coli* at a dose of 10 bacteria per macrophages or with various TLR ligands. Media were harvested for ELISA to measure IFN-β concentration. Cells were harvested to isolate total RNA for qRT-PCR analysis on IFN-β expression. **A.** The effects of p38 and JNK inhibition on IFN-β production by *Mkp-1*$^{+/+}$ and *Mkp-1*$^{-/-}$ BMDM following 6 h of *E. coli* stimulation. **B.** The effects of p38 and JNK inhibition on IFN-β production by *Mkp-1*$^{+/+}$ and *Mkp-1*$^{-/-}$ BMDM following 6 h of LPS stimulation (100 ng/ml). **C.** Kinetics of IFN-β production by *E. coli*-stimulated *Mkp-1*$^{-/-}$ and *Mkp-1*$^{+/+}$ BMDM in the presence and absence of p38 inhibitor. BMDM (10^6 cell) were cultured in 1 ml medium in 12 well plates. **D.** Kinetics of IFN-β mRNA induction in *Mkp-1*$^{-/-}$ and *Mkp-1*$^{+/+}$ BMDM by *E. coli* in the presence and absence of p38 inhibitor. **E.** The effect of SB203580 on the IFN-β mRNA expression

in *Mkp-1*$^{-/-}$ and *Mkp-1*$^{+/+}$ BMDM stimulated with *E. coli* or LPS for 3 h. BMDM (9×10^5 cell) were cultured in 3 ml medium in 60 mm plates. **F.** The effect of SB203580 on the IFN-β mRNA expression in *Mkp-1*$^{-/-}$ and *Mkp-1*$^{+/+}$ BMDM transfected with 1.8 μg poly (I:C) or 1.8 μg herring sperm DNA for 3 h. BMDM (9×10^5 cell) were cultured with 3 ml of medium in 60 mm plates were transfected with the indicated amounts of nucleic acids using polyethylenimine. Data in A, B, and C are presented as mean ± SE (n=3) of the IFN-β concentrations. Data in D, E are presented as mean ± SE (n=3) of fold change over the average levels in unstimulated *Mkp-1*$^{+/+}$ cells. Data in F are presented as mean ± SE (n=3) of fold change over the average levels in mock-transfected (with polyethylenimine) *Mkp-1*$^{+/+}$ macrophages. *, $p<0.05$, compared to *E. coli* or TLR ligand-stimulated *Mkp-1*$^{+/+}$ cells in their respective treatment group (t-test). ‡, $p<0.05$, compared to *E. coli* or TLR ligand-stimulated *Mkp-1*$^{-/-}$ cells in their respective treatment group (t-test). #, $p<0.05$, compared to SB203580-pre-treated, *E. coli*-stimulated *Mkp-1*$^{-/-}$ cells (t-test).

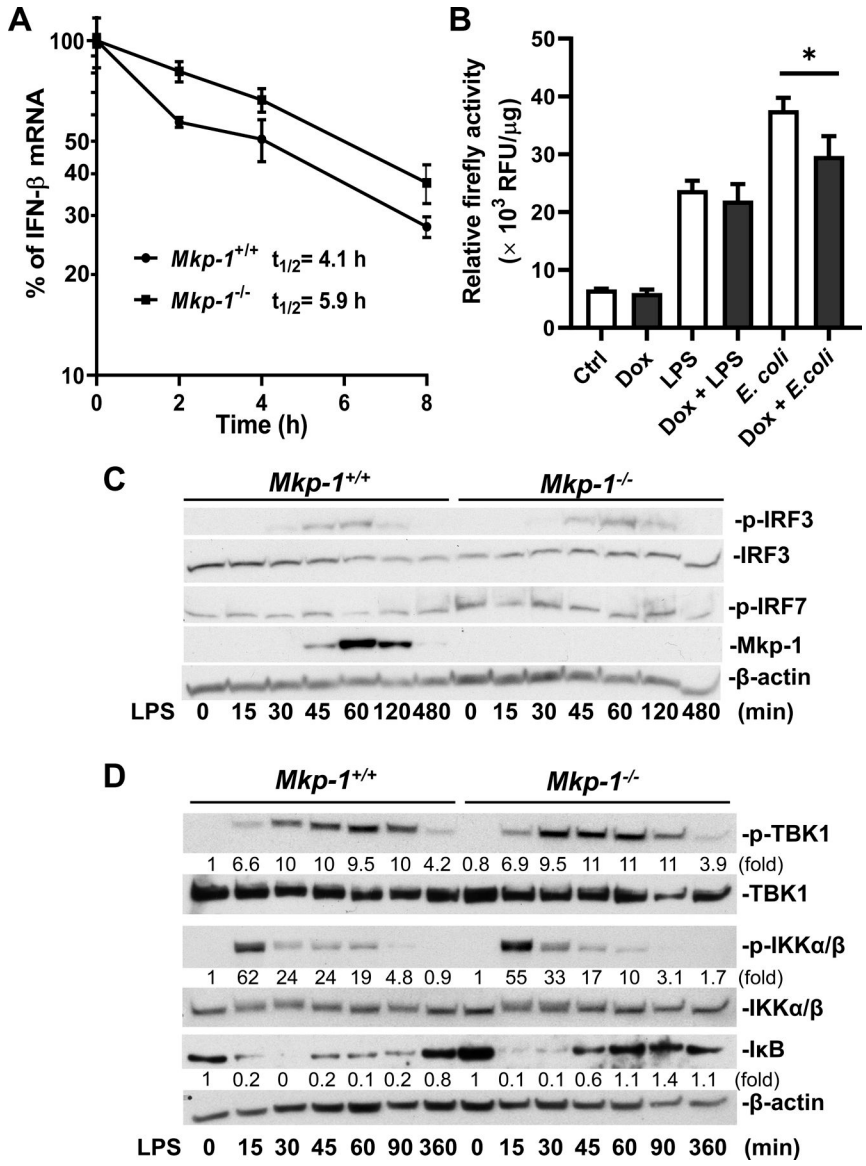

Figure 8. Mkp-1 modestly shortened the stability of IFN-β mRNA but had little effect on IFN-β promoter activity or upstream signaling.

A. Decay of IFN-β mRNA in *E. coli*-stimulated *Mkp-1*$^{+/+}$ and *Mkp-1*$^{-/-}$ BMDM after the addition of actinomycin. *Mkp-1*$^{+/+}$ and *Mkp-1*$^{-/-}$ BMDM (5×10^6 cells on 60 mm plates in 3 ml medium) were first stimulated with heat-killed *E. coli* for 2 h. Actinomycin D was then added into the culture medium (time 0) to a concentration of 2 μg/ml. Total RNA was harvested from the cells after 2, 4, and 8 h. IFN-β mRNA levels were quantified by qRT-PCR to assess IFN-β mRNA decay. IFN-β mRNA levels were normalized to 18S ribosomal RNA. The average levels of IFN-β mRNA at time 0 (no actinomycin D treatment) was set as 100%. The remaining mRNA levels (%) at other time points were calculated relative to the average level of the same genotype at time 0, and presented in the graph as mean ± SE (n=3). Note, y-axis is set in log scale. The half-life ($t_{1/2}$) of IFN-β mRNA were calculated using the formula $N(t) = N_0\, e^{-\lambda t}$, where $t_{1/2} = \frac{\ln(2)}{\lambda}$, $N(t)$ represents

level at time t, N_0 represents level at time 0. **B.** The effect of Mkp-1 over-expression on IFN-β promoter activity. RAW264.7 cells stably integrated with a Tet-ON Mkp-1 expression cassette (Clone 22) were treated with 100 ng/ml overnight or left untreated. Cells were either stimulated with LPS (100 ng/ml) or with heat-killed *E. coli* at a dose of 10 bacteria per macrophage for 6 h or left unstimulated. Cells were harvested to measure luciferase activity. The activity was normalized to lysate protein contents. Values are expressed as mean ± SE (n=4). *, $p<0.05$ (t-test). **C.** The effect of *Mkp-1* deficiency on phosphorylation of IRF3 and IRF7 following LPS stimulation. *Mkp-1*$^{+/+}$ and *Mkp-1*$^{-/-}$ BMDM were stimulated with 100 ng/ml LPS for the indicated times and harvested for Western blot analysis using antibodies against phosphor-IRF3, IRF3, phosphor-IRF7, and Mkp-1. The membrane was stripped and blotted using an antibody against β-actin to control for sample loading. **D.** The effect of Mkp-1 deficiency on TBK1 and IKKα/β activation following LPS stimulation. *Mkp-1*$^{+/+}$ and *Mkp-1*$^{-/-}$ BMDM stimulated with 100 ng/ml LPS were analyzed by Western blotting using antibodies against phospho-TBK1, TBK1, phosphor-IKKα/β, IKKα/β, and IκB. The membrane was stripped and blotted using an antibody against β-actin to control for sample loading. The densities of the individual bands were quantitated by densitometry. The phosphorylated protein was normalized to total protein. IκB was normalized to β-actin. The fold change in protein phosphorylation (TBK1 or IKKα/β) or protein level (IκB) was calculated relative to the value in unstimulated *Mkp-1*$^{+/+}$ cells and is marked underneath each lane. Representative results were presented in **C** and **D**.

Table I.

Morbidity sepsis score (MSS) to assess the severity of disease

Variable	Score	Description
Appearance	0	Coat is smooth
	1	Patches of hair piloerected
	2	Majority of back is piloerected
	3	Piloerection may or may not be present, mouse appears “puffy”
	4	Piloerection may or may not be present, mouse appears emaciated
Level of consciousness	0	Mouse is active
	1	Mouse is active but avoids standing upright
	2	Mouse activity is noticeably slowed. The mouse is still ambulant.
	3	Activity is impaired. Mouse only moves when provoked, movements have a tremor
	4	Activity severely impaired. Mouse remains stationary when provoked, with possible tremor
Activity	0	Normal amount of activity. Mouse is any of: eating, drinking, climbing, running, fighting
	1	Slightly suppressed activity. Mouse is moving around bottom of cage
	2	Suppressed activity. Mouse is stationary with occasional investigative movements
	3	No activity. Mouse is stationary
	4	No activity. Mouse experiencing tremors, particularly in the hind legs
Response to stimulus	0	Mouse responds immediately to auditory stimulus or touch
	1	Slow or no response to auditory stimulus; strong response to touch (moves to escape)
	2	No response to auditory stimulus; moderate response to touch (moves a few steps)
	3	No response to auditory stimulus; mild response to touch (no locomotion)
	4	No response to auditory stimulus. Little or no response to touch. Cannot right itself if pushed over
Eyes	0	Open
	1	Eyes not fully open, possibly with secretions
	2	One eye at least half closed, possibly with secretions
	3	Both eyes half closed or more, possibly with secretions
	4	Eyes closed or milky
Respiration rate	0	Normal, rapid mouse respiration
	1	Slightly decreased respiration (rate not quantifiable by eye)
	2	Moderately reduced respiration (rate at the upper range of quantifying by eye)
	3	Severely reduced respiration (rate easily countable by eye, 0.5 s between breaths)
	4	Extremely reduced respiration (>1 s between breaths)
Respiration quality	0	Normal
	1	Brief periods of labored breathing
	2	Labored, no gasping
	3	Labored with intermittent gasps
	4	Gasping